

Remarks

By this paper, claims 1, 3, 5-19, 28, 29, 31, 32, and 35 are pending in the application. All claims stand rejected. New claims 36-52 are added commensurate with the scope of the invention. Support is found for claims 38-52 in paragraphs [0031] and [0032] of the published application. Filed concurrently herewith is a Request for Continued Examination. Reconsideration in view of the marks presented below is requested.

Section 112, first paragraph

Claims 1, 3, 5-19, 28, 29, 31, 32, and 35 stand rejected under 35 U.S.C. § 112, first paragraph.

The Office Action asserts that a person of ordinary skill in the art would have to undergo clinical trials to measure and develop a criterion to differentiate between different individuals. However, this is incorrect as a substantial body of work has been conducted prior to the filing date of the pending application in the fields of biology, biomedical engineering, diagnostic medicine, photo optics, and medicine to identify individuals. Indeed, a tremendous amount of scholarly studies, clinical trials, research and development, and productization has been conducted in the biometrics field for several decades beginning in earnest in the early 1970's. References are provided with this paper as evidence of the information available to one of skill in the art.

The pending application advances the field of biometrics through the principle of superposition to combine in a layered approach a variety of biological measurements to produce a unique biometric signature sufficient for security

purposes. Individually, each element may in and of itself be inadequate to produce sufficient selectivity, but taken in composite these elements raise the statistical probabilities of uniqueness to an acceptable level. Thus, layering biometric markers provides a statistically significant individual identification. This process is much the same as employed by law enforcement to produce a description of a suspect, where such biometric markers as gender, height, age, color, scars, eye color, etc., are used. Mathematically, multivariate statistical analysis is used to combine multiple variables into a single composite result. See, for example, Sam Kash Kachigan, *MULTIVARIATE STATISTICAL ANALYSIS* (2nd ed., Radius Press 1991). Each trait alone is insufficiently specific for security-based identification applications. A trait that identifies the gender of an individual will immediately reduce the subset of consideration by approximately 50 percent, still leaving a requirement for further delineation of the population under consideration. Add a second trait, such as race, and the sub-population is further reduced. Add a third and a forth and as many as necessary and the population can be effectively reduced to a high probability of containing only the subject of interest.

Authentication by Heartbeat

The Office Action states that:

"[T]he applicant does not provide details on how the particular biometric features of the use of authentication by heartbeat and other live biological traits are unique to a particular group of people or to an individual. Without such details, one skilled in the art would be required to engage in undo experimentation in order to practice or use the invention. A person of ordinary skill in the art would have to undergo clinical trials to measure and come up with a criterion to differentiate between different individuals."

Page 3, first paragraph.

One skilled in the art would be able to reduce the disclosed invention to practice without undue experimentation. A person of ordinary skill in the art would have access to sufficient information to produce a layered biometric measurement based on the application's teachings.

The plethysmographic measure of an individual's heartbeat contains a wealth of biological information, much of which is at least at some level unique to the individual. See, Matthew J. Hayes & Peter R. Smith, Quantitative Evaluation of Photoplethysmographic Artefact Reduction For Pulse Oximetry 138-147 (Proc. SPIE Vol. 3579, Biomedical Sensors, Fibers, and Optical Delivery Systems, January 1999). The presence of a heartbeat first indicates the live and living nature of the test subject. One of the major drawbacks to biometric identifying, techniques such as fingerprints and retinal scans, is the possibility that these measures can be taken on deceased subjects. Thus, fingerprints and retinal scans alone in the absence of "layering" with other living biological traits can be and are foiled.

The Rate of Change of the "up-slope of the heartbeat" conveys information about the long-term general health and physiology of the subject. Unlike the down-slope of the heartbeat, the up-slope is primarily governed by electrical signals from the nervous system of the body. The frequency of occurrence of the heartbeat (heart rate), changes dramatically with the level of exertion and emotional state of the subject. The change in the time base of the cardiac cycle due to this change in heart rate, however, is manifest in a variation of the down-slope, with the up-slope remaining essentially unchanged. See, Udo J. Scholz et al., Multivariate Spectral Analysis of the Beat-To-Beat Sampled Cortical NIRS-Signals and the Heart Rate

Variability 106-111 (Proc. SPIE Vol. 3566, Photon Propagation in Tissues IV, December 1998).

The stability of the nervous system is quite good in the long term and provides a repeatable biometric marker. Anecdotally, should variability of the nervous system cause irregular heart beats, an even more unique signature of the cardiac cycle of the subject is established and serves as an even stronger biometric marker.

The presence and location of the dicrotic notch indicate the resilience and function of the valving system of the heart within the individual. The presence and depth of the dicrotic notch are a good indication of the age of the individual. See, S.A.A.P. Hoeksel et al., *Detection of Dicrotic Notch in Arterial Pressure Signals*, 13(5) J. Clin. Monit. 309 (1997). Younger test subjects who maintain a pliable nature to the cardio-vascular system have a stronger, well-pronounced notch. Conversely, as the human body ages, the pliability of the cardio vascular system begins to stiffen, thus reducing the presence and depth of the notch. Certain defects and disease modalities can also affect the position and depth of the notch; but much the same as irregular heartbeats, the signatures established by these modalities only lend to the uniqueness of the marker and strengthen its use as a biometric measure.

Variability due to physical stress, emotion level, amount of physical activity, time of day, and health of the individual are generally exhibited in more than one characteristic of the cardiac signature. For example, the heart rate will increase due to level of activity or emotional state, but concurrent to the increase of heart rate is an increase in the respiration rate. These two increases occur simultaneously and, when taken in concert with each other, can be used to ratiometrically normalize out

the short-term variations due to changing physical states. In fact, it is the scientific method of normalization that allows most scientific measurements to be made. See, *Waveform Normalization in a Medical Device*, U.S. Patent No. 6,266,566 (filed May 21, 1999) (issued July 24, 2001). For example, in the measure of pulse oximetry, a second wavelength of light is used to normalize the prorated quantity of blood in the finger tip. See, Anna Cysewska-Sobusiak, *Noninvasive Monitoring of Arterial Blood Oxygenation with Spectrophotometric Technique*, 311-322 (Proc. SPIE Vol. 1711, High-Performance Optical Spectrometry, 1993). In dosing medications, weight and size are used to normalize the proper dosage. In determining ideal body weight, height and bone structure are used to normalize appropriate individual weight. In the case of this biometric marker, respiration is used to normalize heart rate.

Despite the popular belief, pacemakers do not maintain constant heart rates. The Office Action's assertion that "... multiple individuals with the same pacemaker will all have the same heart rate", is in error. Office Action dated March 26, 2003, at page 3, paragraph 2. Pacemakers continuously monitor the electrical impulses coming from the individual's nervous system and respond accordingly to pre-set algorithms. If the individual's body is in a state of exertion, the pacemaker will respond to various physiological signals and move to increase the heart rate. See, *Artificial Pacemaker*, http://en.wikipedia.org/wiki/Artificial_pacemaker (last visited January 26, 2007) and *Rate-Responsive Pacing Systems*, Medtronic, Inc., http://www.medtronic.com/servlet/ContentServer?pagename=Medtronic/Website/StageArticle&ConditionName=Bradycardia&Stage=Treatment&Article=brady_art_rate_responsive (last visited January 26, 2007). Otherwise, an individual with a pacemaker

would have insufficient blood flow for even the simple task of ascending a flight of stairs. In fact, most pacemakers only stimulate the heart a small percentage of the time, often less than 10 percent.

Pacemakers are programmed by the cardiologist at the time of placement and periodically adjusted to the individual's needs. In a very real sense, each individual pacemaker is uniquely programmed with its own signature. The Applicants strongly submit that a pacemaker will greatly enhance the ability to appeal to the cardiac signature as a biometric marker, rather than diminish from it as suggested in the Office Action.

Based on the foregoing, the Applicants respectfully submit, that with the body of knowledge available at the time, it is well within the scope of one of ordinary skill in the art to use a heartbeat to assist in uniquely identifying a particular group of people or an individual.

Authentication by Bone Density

The density of the bones can be affected by a number of physiological issues; primary among these are gender and age. See, L. Leichter et al., *Effect of Age and Sex on Bone Density, Bone Mineral Content and Cortical Index*, 156 Clin. Orthop. Relat. Res. 232 (May 1981) and Paul D. Miller, M.D., *Assessing Fracture Risk: Which Factors are Clinically Most Important*, Medscape Today, http://www.medscape.com/viewarticle/493478_1 (last visited January 26, 2007). As the body ages, it naturally loses density within the bones. In advance age, this loss of bone density is a direct attributing factor to the high incidence of hip fractures in elderly persons. This loss of bone is generally more prevalent in post menopausal

women who tend to lose calcium at much higher rates than their younger counterparts. Using bone density as a biometric marker would, for example, make it virtually impossible for a young man to pass himself as an older man or women.

Authentication by Bone and Tissue Structure

The structure of the human skeleton in many ways is very unique to the individual. For example, bones that have been broken and subsequently healed leave a life-long (and well beyond) signature. Indeed, forensic science can determine even hundreds of years after death the nature of an injury and the age at which the injury occurred. See, Shelley L. Smith, *Attribution of Hand Bones to Sex and Population Groups*, 41(3) J. Forensic Sci. 469 (1996). Additionally, certain disease modalities generate unique bone structures within the human bone structure. For example, certain types of cancer and heart disease can cause clubbing of the fingers. Arthritis causes inflammation and swelling of the joints. Finally, the size of the bone structure is a good marker of age and gender. Children have small bones; women generally have smaller bones, and so on.

Heat Quantity and Flux

One of the primary distribution and regulation mechanisms of heat within the body is the blood flow. Blood vessel dilation to increase venting circulation is the primary modality by which the body vents internally generated heat. Monitoring the sub-dermal heat signature of an individual enables one skilled in the art to "map" the vascular structure of the sub-dermal system. Blood vessels within the human body grow and distribute along the mathematical principle of fractals. Fractals is the branch of mathematics used to describe organized random events. A good example

of this principle in nature is the growth of oak trees. From a distance, all oak trees of a given variety have a similar appearance. They look like oak trees. Up-close inspection, however, reveals that each tree has a unique branch structure. Similarly, the vascular structure within an individual follows general human structures of veins and arteries, but upon closer inspection, each individual's vascular structure is unique. Using heat signatures to map out the vascular structure renders a very specific signature and provides an excellent biometrics marker. Additionally, heat indicates a living subject and can be layered with other biometric markers to provide a statistically significant individual identification.

Electrical Characteristics

Electrical capacitance and impedance are used extensively in characterizing the physiology of the body. A good example is the use of electrical impedance to determine level of blood constituents, such as red blood cell content (hematocrit). See, *Method and Apparatus for Noninvasively Determining Hematocrit*, U.S. Patent No. 5,526,808 (filed April 20, 1995) (issued June 18, 1996). The nature of the fluids and tissue matter in the body affect the frequency response of low level, electrical currents passing through the body. The body's natural characteristics act to tune the electronics in much the same way as a radio receiver tunes in a desired radio signal. One skilled in the art can easily measure the capacitance of an individual and, from it, derive blood parameters. The hematocrit, for example, is a good indication of general state of health. It also correlates well to environmental conditions. For example, a subject living at altitude, say in Salt Lake City, Utah, will on average have a hematocrit 5 percent points higher than a subject living at sea level. Hematocrit is

the primary test for doping violations in sporting events. It should be noted that hematocrit can also be measured optically.

Each biometric identifier or trait, alone, may be insufficient to adequately identify an individual. However, a plurality of such identifiers or traits layered together in composite provide sufficient reliability in identifying an individual.

Section 112, second paragraph

Claims 3, 5-8, 17, 29, 31, and 32 stand rejected under 35 U.S.C. § 112, second paragraph. As amended herein, the rejected claims are now in compliance. Reconsideration is requested.

Section 101

Claims 20-27 stand rejected under 35 U.S.C. § 101. Claims 20-27 have been canceled herein.

Section 103

Claims 1, 16, 18-19, 28, 31, and 32 stand rejected under 35 U.S.C. § 103(a) as being unpatentable over U.S. Patent No. 4,993,068 to Piosenka ("Piosenka") in view in view of U.S. Patent No. 5,719,950 to Osten et al. ("Osten") and further in view of EP 197810 to Vanoni ("Vanoni").

Claim 1 is amended herein to recite "reading a first unique, heartbeat waveform of an individual." Support is found for this limitation in Figures 1 and 2 and the accompanying text.

The Office Action recites to Vanoni for teaching the reading of a Doppler signal waveform from blood flowing in a human artery. Vanoni teaches emitting signals in the direction of an artery and detecting and comparing resulting Doppler signals. Vanoni, abstract.

Doppler measurements are of use in the medical industry to aid in the determination of blood flow through various parts of the body. An example is the measure of blood flow through a natural fistula in a hemo-dialysis patient. Transonic System, Inc. produces an instrument that in fact makes this very measurement. However, Doppler measurements are not capable of reading a heartbeat waveform as claimed.

Doppler technology measures the velocity of an object. To use Doppler measurements as a biometric marker, however, presents several significant difficulties. The primary difficulty of Doppler is in attempting to normalize the measurement. Doppler measurements are made in the frequency domain as energy waves, generally ultrasonic, where the frequency shifts in proportion to the speed of the object from which they are reflected. A mathematical integration is required to translate this information back into the time domain to determine information concerning the cardiac cycle. Fundamental calculus teaches that an integration operation results in an undetermined constant of integration "c" that can only be determined via a boundary condition. This is where the difficulty presents itself, as it is difficult to determine a reliable boundary condition for the vascular flow of blood.

In Vanoni, the velocity is of the blood movement within an artery. It is not possible to determine absolute amplitudes with Doppler techniques, as such

techniques are incomplete without a well-defined boundary condition. All that can be measured is the rate of change in the blood movement, not the total amount of blood movement. This means that the date mined from a Doppler measurement is at best a subset of the information gathered from an actual amplitude waveform measurement. Accordingly, it is not possible to make a full waveform measurement from a Doppler technique. Thus, not only does Vanoni not teach how to measure and analyze a heartbeat waveform, it simply is not possible with the disclosed techniques of Vanoni.

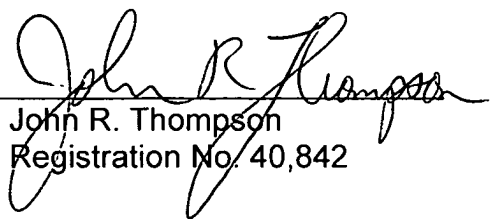
Piosenka, Vanoni, and Osten all fail to disclose reading and analyzing a heartbeat waveform and cannot obviate claim 1. "To establish *prima facie* obviousness of a claimed invention, all the claim limitations must be taught or suggested by the prior art." MPEP § 2143.03. Independent claims 9, 11, 16, 28, and 35 recite limitations for reading a heartbeat waveform and likewise represent patentable subject matter. The remaining claims depend from their respective independent claims, and are likewise allowable by virtue of that dependency. Reconsideration is respectfully requested.

In view of the foregoing, all claims are believed to be in condition for allowance. A Notice of Allowance is respectfully requested.

Respectfully submitted,

Ensign Holdings

By


John R. Thompson
Registration No. 40,842

STOEL RIVES LLP
One Utah Center Suite 1100
201 S Main Street
Salt Lake City, UT 84111-4904
Telephone: (801) 328-3131
Facsimile: (801) 578-6994

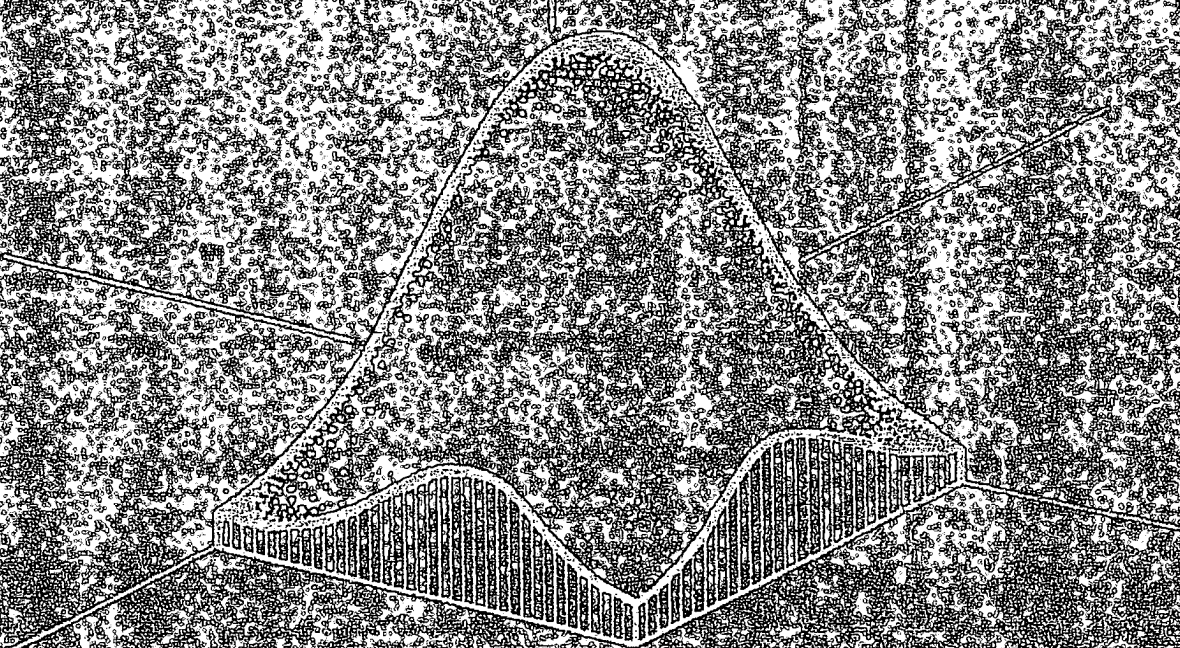
Best Available Copy

SECOND EDITION

MULTIVARIATE
STATISTICAL
ANALYSIS

A Conceptual Introduction

KACHIGAN



MULTIVARIATE STATISTICAL ANALYSIS

**Copyright © 1991, 1986, 1982 by Sam Kash Kachigan.
All rights reserved.**

No part of this book can be reproduced without the prior written permission of the
publisher: RADIUS PRESS, P.O. Box 1271, FDR Station, New York, NY 10150.

Manufactured in the United States of America.

Library of Congress Cataloging-in-Publication Data

Kachigan, Sam Kash.

Multivariate statistical analysis : a conceptual introduction /
Sam Kash Kachigan. — 2nd ed.

p. cm.

Includes bibliographical references and index.

ISBN 0-942154-91-6

1. Multivariate analysis. I. Title.

QA278.K32 1991

519.5'35—dc20

91-52869

CIP

0-942154-91-6

15 14 13 12 11 10

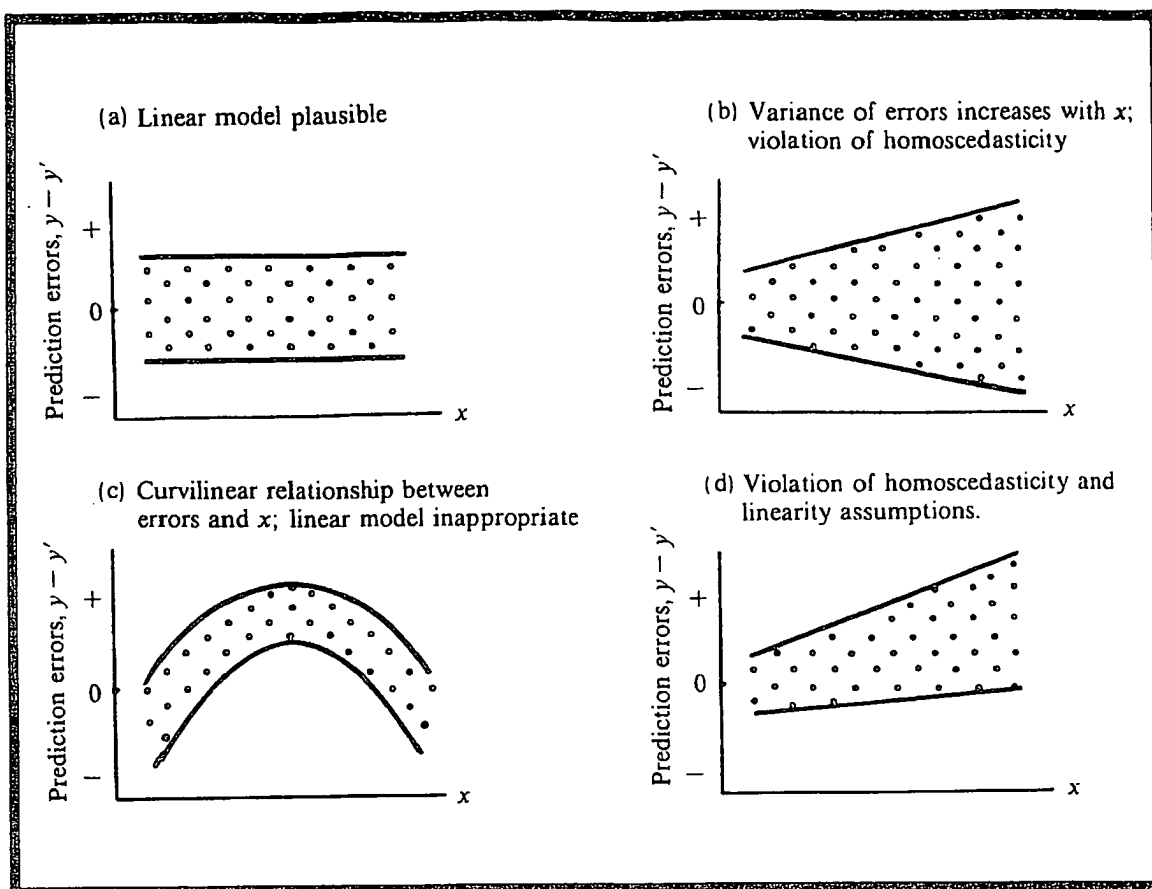


Figure 8 Examples of residual prediction error plots and likely interpretations.

8. Multiple Regression

Multiple regression is an extension of the concept of simple regression. Rather than using values on one predictor variable to estimate values on a criterion variable, we use values on *several* predictor variables. In using many predictor variables instead of just one, our aim is to reduce even further our errors of prediction; or, equivalently, to account for more of the variance of the criterion variable.

The input data for a multiple regression analysis is similar to that for a multiple correlation analysis; namely, a random sample of objects measured on some criterion variable of interest, as well as on k predictor variables. While the multiple correlation analysis requires that the predictor variables are random variables—as opposed to being determined by the researcher—there are multiple regression models to cover both types of situations.

An example of the type of problem to which multiple regression analysis lends itself would be the prediction of college grade point average based on predictor variables such as high school grade point average, aptitude test scores, household income, scores on various entrance exams, etc. A number of other examples of the application of multiple regression analysis will be

introduced at the end of the chapter, after the basics of the technique have been studied.

Multiple regression equation. The multiple regression equation will be recognized as similar to the simple regression equation, but instead of a single predictor variable x we have several predictor variables x_1, x_2, \dots, x_k . The general form of the equation is

$$y' = a + b_1 x_1 + b_2 x_2 + \dots + b_k x_k \quad (9)$$

where y' is the predicted value of the criterion variable and the values of a and the b coefficients must be determined from the sample data. Since it is based on sample observations, equation (9) must be thought of as an estimate of the true but unknown population equation

$$\mu_y = a + \beta_1 x_1 + \beta_2 x_2 + \dots + \beta_k x_k \quad (10)$$

Equations (9) and (10) do not represent straight lines as in the case of simple regression where we have only one predictor variable, but rather represent *planes* in multi-dimensional space, a concept admittedly difficult to conceive and virtually impossible to portray graphically. However, its application is easy enough.

As in simple regression, the least squares solution is used to determine the best multiple regression equation; i.e., the values of a, b_1, b_2, \dots, b_k that will yield values of y' such that the sum of the squared deviations of the predicted y' values from the actual observed y values— $\sum(y - y')^2$ —is at a minimum. Alternatively, we can think of the least squares solution as that *weighted sum of values on the various predictor variables* that correlates most highly with the values on the criterion variable. For example, if the least squares criterion yielded the following equation for a three-predictor variable problem

$$y' = 24.3 + 7.1x_1 + 6.2x_2 + 91.5x_3$$

we would know that no other equation would yield predictions y' which would correlate more highly with the observed values of y ; or, equivalently, no other equation would result in a smaller value of $\sum(y - y')^2$, the sum of the squared differences between the actual and predicted values of y .

Regression coefficients. The values of b_1, b_2, \dots, b_k in the regression equation $y' = a + b_1 x_1 + b_2 x_2 + \dots + b_k x_k$ are alternatively referred to as *b coefficients* or as *regression coefficients*. In the following section, we will get a better idea of the interpretation, and limits on the interpretation, of the *b* coefficients; where they will be contrasted with *beta* coefficients based on the regression equation in standardized *z* score form.

Quantitative evaluation of photoplethysmographic artefact reduction for pulse oximetry

Matthew J. Hayes¹ and Peter R. Smith

Optical Engineering Group, Department of Electrical and Electronic Engineering,
Loughborough University, Loughborough, Leicestershire, LE11 3TU, UK

ABSTRACT

Motion artefact corruption of pulse oximeter output, causing both measurement inaccuracies and false alarm conditions, is a primary restriction in the current clinical practice and future applications of this useful technique. Artefact reduction in photoplethysmography (PPG), and therefore by implication in pulse oximetry, is demonstrated using a novel non-linear methodology recently proposed by the authors. The significance of these processed PPG signals for pulse oximetry measurement is discussed, with particular attention to the normalisation inherent in the artefact reduction process. Quantitative experimental investigation of the performance of PPG artefact reduction is then utilised to evaluate this technology for application to pulse oximetry. Whilst the successfully demonstrated reduction of severe artefacts may widen the applicability of all PPG technologies and decrease the occurrence of pulse oximeter false alarms, the observed reduction of slight artefacts suggests that many such effects may go unnoticed in clinical practice. The signal processing and output averaging used in most commercial oximeters can incorporate these artefact errors into the output, whilst masking the true PPG signal corruption. It is therefore suggested that PPG artefact reduction should be incorporated into conventional pulse oximetry measurement, even in the absence of end-user artefact problems.

Keywords: photoplethysmography, pulse oximetry, artefact reduction, motion artefact

1. INTRODUCTION

Pulse oximetry^[1] is the dominant non-invasive method for determination of arterial oxygen saturation of haemoglobin, which is mandatory under anaesthesia in operating theatres worldwide. The technique is well established as an early warning for hypoxia during anaesthesia, recovery and intensive care^[2]. The measurement relies on the knowledge that haemoglobin and oxy-haemoglobin absorb light to varying degrees as a function of wavelength^[3]. Illumination of blood by two light sources of differing wavelengths produces an absorption contrast that is dependent on the relative concentrations of the haemoglobin species, and therefore the oxygen saturation. Pulse oximeters utilise photoplethysmography^[4] (PPG), the technique of monitoring the human cardio-vascular pulse wave by observation of the dynamic optical absorption induced by pulsating arterial blood in well-perfused peripheral sites, to differentiate between absorption by dynamic arterial blood and other tissue constituents that remain static. Spectroscopic determination of the oxygen saturation using PPG signals implies an inherent independence of the optical properties of the skin, bone and non-pulsatile tissue.

Corruption of PPG signals can arise from inadvertent measurement of ambient light (ambient artefact) and from voluntary or involuntary subject movement (motion artefact). The relatively small dynamics from arterial blood pulsations are easily obscured by artefacts, leading to errors in the interpretation of these signals for pulse oximetry^[5]. Although oxygen saturation measured by pulse oximetry has demonstrated good correlation with invasive blood gas measurements under controlled operating conditions^[6], many authors have highlighted inaccuracies during normal clinical practice^[7,8]. These errors can occur because of limitations in the empirical calibration algorithms used^[9], or because of poor PPG signal to noise ratio caused by low perfusion states^[10] or artefact^[11]. The problem of artefact is especially severe for monitoring exercising subjects, foetuses and children, and in ambulatory studies. In addition, the major proportion of oximeter false alarm conditions can also be attributed to motion artefact^[12], accounting for the predominant end-user perception of the problem.

¹ For further information contact –

Email: M.J.Hayes@Lboro.ac.uk

Tel: +44 (0)1509 228111

WWW: <http://www.lboro.ac.uk/departments/el/research/optics/>

However, transient or less severe artefact corruption of the PPG signals can also cause significant errors in pulse oximeter output that, because of the averaging used in most commercial devices, may introduce unnoticed output errors^[13]. Whilst the accuracy of pulse oximeters has been empirically demonstrated to decrease under conditions of subject movement^[14,15], therefore restricting the applicability of this useful technique, it can be shown that this is a direct result of motion artefact corruption of the underlying PPG signals^[13,16].

Removal of signal artefacts cannot be easily performed by signal processing methods, because of several key features of observed artefact corruption:

- The artefact may vary in size up to several orders of magnitude larger than the arterial pulsations, creating a severe signal-to-noise ratio problem. In addition, the relatively small size of arterial pulsations in comparison to the overall magnitude creates a dynamic range problem for any digital signal-processing attempt.
- In the general case, there is no knowledge, explicit or implied, which can be used to separate the artefact from the PPG signal, either spectrally or temporally.
- The artefact and PPG signals can commonly be observed to be statistically dependent, a condition that hampers more sophisticated signal-processing solutions.

2. EXTANT SOLUTIONS

Existing commercial attempts to address the problem of artefact have concentrated on the problem of motion artefact, assuming that reported errors due to ambient artefact^[17,18] are due to unrealistic extremes that should be avoided in clinical practice. It is unfortunate to observe the lack of purely academic literature available on this subject, with the bulk of extant solutions published only in the patent literature and concentrating on the reduction of oximeter false alarms in a clinical environment. These methodologies can be broadly divided into four categories:

1. Signal processing solutions, either spectral^[19] or correlation cancellation^[20-22].
2. Recognition of artefact by either feature based recognition of corrupt pulses^[23,24] or identification of interpretation errors (pulse rate^[13,14] or oxygen saturation^[25]).
3. Modification of the calibration scheme to maximise insensitivity to artefact^[26,27].
4. Cancellation of artefact by intensity control of a pair of sources^[28].

Signal processing solutions utilise a-priori assumptions about the nature of expected PPG signals, commonly spectral^[19], statistical^[22], or concerning the degree of correlation with signals from another transducer^[20,21]. The success of these attempts to remove artefact from received signals depends entirely on the validity and scope of the assumptions. Although some success in the reduction of false alarms has been reported^[16,29], the lack of generality of the assumptions makes it difficult to assess the performance of these techniques for improving the output accuracy under conditions of transient or less severe artefact. In addition, the inherent assumption of signal processing solutions in general is that motion artefact is manifested as an additional intensity, or additive noise term. It has been demonstrated^[30] that observation of PPG signals under typical artefact producing forces casts doubt on this hypothesis, which would preclude the measured dynamics from being affected by the artefact. This questions both the accuracy and physiological relevance of PPG signals that have been processed in this manner.

Recognition of artefact is an inherently digital process that has no effect on output accuracy during periods of slight artefact and fails to provide any data during extended periods of artefact, such as exercise testing. Although this methodology fails to address the fundamental problem of output inaccuracies due to artefact, it can significantly reduce the occurrence of false alarms in a clinical environment^[31], therefore alleviating the end-user perception of the artefact problem.

Modification of the calibration scheme can provide a degree of insensitivity to slight artefact, but the intrinsically wide dynamic range of PPG signals makes it difficult to implement devices that are insensitive to severe artefact, which could easily dominate the available digital precision. One method^[27] assumes that artefact affects the received intensity in a proportional manner, the cancellation of which ideally requires a three wavelength calibration. Although there is no theoretical or experimental justification of this technique available in the open literature, the model is certainly more general than an additive noise model.

Cancellation of artefact has been proposed^[28] by subtraction of a pair of received signals whose average levels are largely identical, maintained by dynamic control of the source intensities. Again, the inherent assumption of this technique is that artefact can be modelled by an additional intensity, in this case one that is synchronous for all wavelengths and whose size is proportional to the average intensity level. Whilst there is no direct evidence to date as to the success of this technique, it is likely that the additive assumption will be the limiting factor in determining the achievable level of artefact reduction.

3. NON-LINEAR ARTEFACT REDUCTION

A non-linear artefact reduction methodology can circumvent many of the theoretical and practical problems highlighted, by inversion of a heuristic model describing the optical interaction with tissue and the effects of motion artefact^[30]. The primary assumption of this model is that any received light that has been transmitted through (or reflected from) the human anatomy may be separated into components from distinct and independent optical paths. We examine the case where a number of sources are used in conjunction with a single receiver to generate one or more PPG signals. The received intensity, as a function of time, t , and wavelength, λ , is modelled by

$$I(t, \lambda) = \sum_{j=1}^n I_j [\beta_j(t, \lambda) + \gamma_j(t, \lambda)], \quad (1)$$

where j labels a light-source of intensity I_j and β_j , γ_j are coupling coefficients that identify optical paths and encompass all geometric, temporal and spectral properties of both the sensor and illuminated anatomy. The coefficients γ are interpreted as light coupled via pulsatile vascular tissue, whilst those labelled β account for light coupled from non-pulsatile tissue and other anatomical components. We now attribute the dynamic portion of the pulsatile tissue coupling-coefficient to an underlying physical pulsation, which originates from a dynamic change in illuminated arterial blood volume. Because of the fairly uniform distribution of blood within the peripheral vasculature, this volume change is discernible as a change in the homogeneous and macroscopic optical properties of the tissue, and therefore ultimately as a dynamic optical path length. The Beer-Lambert law, which couples physical path length and effective absorbance into a single definition of optical density, is commonly used in pulse oximetry to assign physical significance to changes in the optical path length^[32], although its applicability is questionable^[33]. We justify its use here by restricting application to the relatively small increments in the pulsatile optical path. Linearisation of the effect of a small increase in blood volume, and therefore in physical path length, enables us to write the dynamic coupling coefficient in terms of its static value and the change in physical path length $\Delta z(t)$ through blood of absorbance $\mu_{blood}(\lambda)$,

$$\gamma_j(t, \lambda) = \gamma_j(\lambda) \mu_{blood}(\lambda) \Delta z(t). \quad (2)$$

We now examine the behaviour of the model under conditions of motion artefact. Excluding physiological dynamics, such as dynamic venous blood volume, the majority of artefacts can be observed to have arisen from changes in the optical probe coupling, either primarily or in conjunction with other effects^[30]. Whilst it is acknowledged that there are other classes of motion artefact, and that physiological dynamics other than arterial pulsations may be interpreted as artefacts in the context of pulse oximetry, the predominance of *probe-coupling* artefacts and the ensuing simplicity of their removal justifies further investigation. Probe-coupling artefact has the effect of modulating all coupling coefficients in an identical manner that does not depend on the source characteristics. This observation suggests that a logarithmic transformation of the received intensity will separate any probe-coupling motion artefact into an additional term that is independent of the source wavelength or intensity. The difference between any pair of non-linear signals will therefore be independent of probe-coupling motion artefact. Consideration of the detailed ordering of terms in this difference, in conjunction with the use of sources whose wavelengths are chosen to exhibit a high degree of contrast between their relative absorption in blood and other tissue constituents, enables us to approximate this difference^[30] as

$$\ln I_j(t, \lambda) - \ln I_k(t, \lambda) \approx \ln \left(\frac{I_j \beta_j(\lambda)}{I_k \beta_k(\lambda)} \right) + \frac{\gamma_j(\lambda) \mu_{blood}(\lambda) \Delta z(t)}{\beta_j(\lambda)}. \quad (3)$$

Examination of equation (3) reveals both static and dynamic signal components, which may be separated with electronic filters. The static component comprises a logarithmic ratio of the equivalent portions of the two received intensities. The dynamic component, however, is independent of both source intensities and any contribution from the source labelled k . It is

noted that the re-normalisation inherent in the non-linear transformation has incorporated static non-pulsatile information into the dynamic term. Interpretation of received light from the j source may therefore be made entirely from the dynamic component of equation (3). Because of the independence from probe-coupling motion artefact, we can say that the j signal has been *equalised* with the use of a *control* source, k . One example of signal dynamics before and after equalisation can be seen in figure 1, which demonstrates the reduction of severe probe-coupling artefact (see section 6 for experimental conditions). Since interpretation of an equalised signal does not require information about the control source, spectroscopic measurement for pulse oximetry can be performed with the two conventional sources and a common control source, used to equalise both signals. A simple two-wavelength calibration can then be performed to determine SaO_2 by consideration of the resulting equalised dynamics only, which comprises a significant engineering simplification over the conventional technique of high-precision measurement of instantaneous intensities. In addition, the non-linear transformations and subtractions can be simply incorporated into the receiver circuitry, obviating the need for complex digital artefact-reduction algorithms.

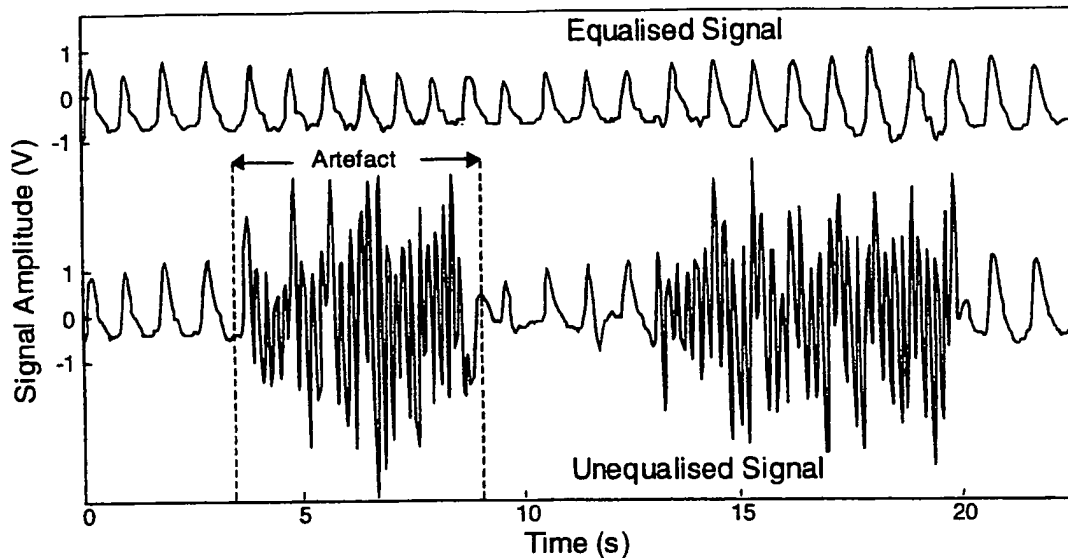


Figure 1 - Demonstration of the reduction of severe probe coupling artefact

4. OXYGEN SATURATION CALIBRATION

Calculation of SaO_2 is conventionally made by computation of a quantity called the *ratio of ratios* (R), which is defined as the ratio of the absorbance of blood at the two wavelengths utilised. Calibration is then performed empirically, employing induced hypoxia experiments^[33]. This calibration maps the ratio of ratios to the calibrated SaO_2 ($S^*100\%$). The ratio of ratios is normally calculated as a ratio of the logarithmic derivatives, or equivalently a ratio of the normalised derivatives of the received intensities,

$$R = \frac{I(t, \lambda_2) \Delta I(t, \lambda_1)}{I(t, \lambda_1) \Delta I(t, \lambda_2)} = \frac{S\mu_{HbO_2}(\lambda_1) + (1-S)\mu_{Hb}(\lambda_1)}{S\mu_{HbO_2}(\lambda_2) + (1-S)\mu_{Hb}(\lambda_2)}. \quad (4)$$

A typical value for R can be obtained by linear regression analysis of an ensemble of data points, a stable method that can easily be applied to digitally sampled signals. We can also calculate the ratio of ratios from a pair of equalised signals, using only the dynamic components,

$$R = \frac{\mu_{blood}(\lambda_1)}{\mu_{blood}(\lambda_2)} = \frac{I_{AC}^{eq}(t, \lambda_1)}{I_{AC}^{eq}(t, \lambda_2)} T_{12}, \quad (5)$$

$$T_{12} = \frac{\gamma(\lambda_2)\beta(\lambda_1)}{\gamma(\lambda_1)\beta(\lambda_2)} \quad (6)$$

Because the additional factor T_{12} is itself a ratio of ratios, comprising of both pulsatile and non-pulsatile components, its numerical value should be stable and relatively independent of specific physiological or geometric conditions. Indeed, this generalisation can be demonstrated to be equivalent to the conventional formulation when the Beer-Lambert law is applied indiscriminately to all optical paths, resulting in a constant factor T_{12} of unity. In the more general case, this factor enables an additional degree of freedom in empirical calibration of the device.

5. QUANTITATIVE EVALUATION OF ARTEFACT REDUCTION

The degree to which a pulse oximeter designed using this methodology would be insensitive to motion artefact would be determined by the degree of artefact independence of equation (3). A comparison between the received intensity before and after equalisation with respect to a suitable control source enables quantification of the degree of artefact reduction achieved by the non-linear methodology. The use of commercial pulse oximetry transmission-mode finger-probes enables experimental creation of realistic artefacts encountered in clinical practice. The commonly utilised wavelengths within these probes are suitable for equalisation, such that the infrared signal may be equalised with respect to the red signal. Although a practical artefact reducing pulse oximeter would require three wavelengths, there are several options for the common control source. A source whose wavelength exhibits a large degree of relative contrast in comparison to both red and infrared wavelengths, such as the blue region, could be used to equalise both measurement wavelengths. Alternatively, the recently proposed use of a pair of near-infrared sources for pulse oximetry^[34] would enable the red region to be used as a control source in a practical device. In this way the scope of this technique, and therefore its suitability for application to pulse oximetry, may be examined.

Unbiased and definitive classification of artefact present within a received PPG signal is not possible in the general case, implying that artefact must be strictly defined within an experimental protocol. Because artefact quantification shares its general principle with artefact recognition, we can again examine the extant solutions in an attempt to identify a suitable artefact recognition method. From the available literature, two possibilities stand out as obvious candidates; namely feature based recognition of corrupt pulses^[23,24] or verification of pulses by comparison with an additional transducer^[13,14,25]. The intrinsically digital classification of pulses can be made quantitative by defining an artefact measure as the proportion of pulsations that have been corrupted within any given data set. Whilst these methods may work well during periods of extended and relatively severe artefacts, they are inherently limited in their sensitivity to both very severe and very mild artefact. Severe artefact causes all pulsations to register as corrupt, whilst mild artefact does not cause severe enough corruption for any artefact recognition to occur. In addition, digital classification of corrupt pulses will result in a highly non-linear relationship between the artefact measure and the observed signal corruption and its effect on pulse oximeter accuracy.

An alternative method of artefact quantification is therefore proposed, based upon control of experimental conditions such that induced artefact is always spectrally separate from the desired PPG signal. This can be achieved easily in practice by performing periodic artefact-inducing movements that have a frequency that is significantly higher than frequencies contained within a clean PPG signal. Whilst this technique would be unsuited to the testing of a signal processing approach to artefact reduction, the non-linear methodology is not dependent on the spectrum of either the artefact or the arterial pulsations. Results from spectrally controlled experiments may therefore be applied to the more general broad-spectrum case. The analogue and continuous nature of spectral quantification techniques can provide an artefact measure that is both linear with respect to the observed signal corruption and equally sensitive to

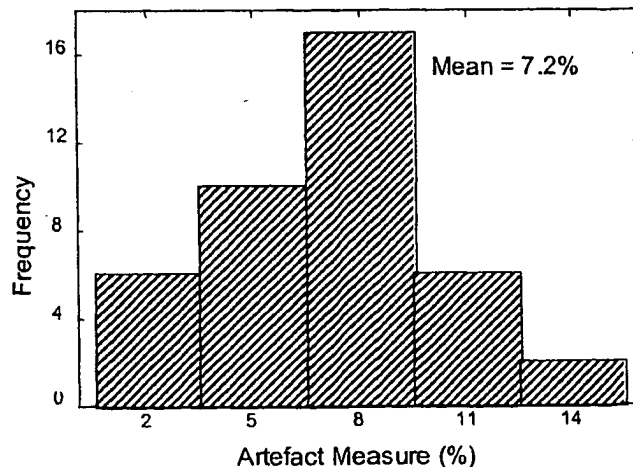


Figure 2 – Distribution of artefact measure for uncorrupted PPG signals

mild and severe artefacts. In addition, the sensitivity of artefact measures to signal variability between subjects is reduced in the frequency domain, simplifying the necessary experimental conditions. In this way it is possible to both recognise and quantify artefact corruption under controlled experimental conditions, whilst maintaining applicability to the general case of possible artefacts encountered in a clinical environment.

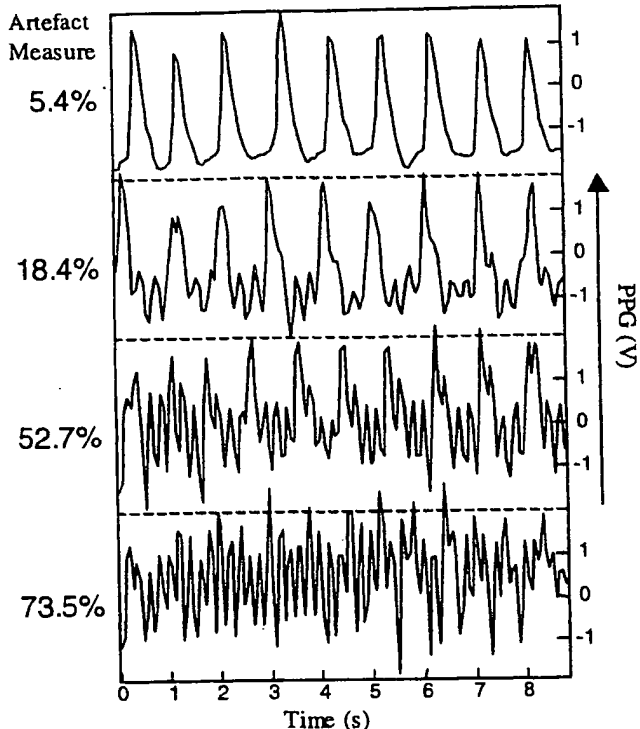


Figure 3 – Artefact quantification

severity of corruption may make it impossible to correctly interpret the signals, and this level roughly represents the digital threshold for classification of individual pulsations. When the measured artefact is 70% or greater, the PPG signal has been completely destroyed and interpretation is now impossible.

6. EXPERIMENTAL METHODOLOGY

The fundamental lower limit on the sensitivity of the spectral artefact measurement precludes the absolute quantification of artefact reduction, unless both equalised and unequalised signals are severely corrupted. Nevertheless, quantification of artefact before and after the equalisation process can still be used as an indication of the effectiveness of the equalisation process under differing experimental conditions. In order to investigate the applicability of the artefact reduction technique, it is first necessary to perform a control experiment, whose results can be used as a basis for comparison with other, more complex situations. In this case, the most appropriate control experiment is the generation of pure probe-coupling motion artefact. The performance of artefact reduction achieved under conditions of pure probe-coupling artefact is a good indicator of the validity of models and assumptions used in obtaining an inversion for artefact reduction. Producing pre-defined movements that can be compared to those likely to occur in clinical practice can simulate more complex artefacts under experimental conditions. The combination of probe coupling and physiological effects that are expected to occur will result in a level of artefact reduction that not only depends on the system performance, but also the origin of the artefacts. In this way we can separate the verification of the reduction of probe-coupling motion artefact from an investigation of the scope of this technique for clinical application to pulse oximetry.

The generation of pure probe coupling artefact is relatively straightforward when using a standard transmission mode finger probe. Pressure applied to the finger probe clip lifts the opto-electronics away from the finger, therefore simulating probe-coupling artefact. Obviously, care must be taken during the experiments not to allow the probe body to exert any pressure on

Statistical observation of the spectra of uncorrupted PPG signals from a range of healthy adult volunteers (25-second data sets, 13 volunteers performing 3 experiments each) was used to identify a suitable spectral artefact quantification. It was discovered that in most cases 90 to 95% of the PPG signal power was contained within a spectral region extending to three times the fundamental frequency, or the subjects heart rate. This leads to a convenient definition of artefact, as the proportion of signal power that has a frequency greater than three times the fundamental. The probability distribution of this artefact measurement when applied to the uncorrupted PPG data (figure 2) shows that, on average, artefact values of around 5 to 10% are to be expected for perfectly clean data. This represents a minimum artefact magnitude, below which any high frequency artefacts cannot be distinguished from the intrinsic PPG signal components at those frequencies. If we induce relatively high frequency artefacts then we expect the proportion of signal power in this spectral region to increase, thus increasing our measure of artefact. This quantitative measurement can be demonstrated by consideration of the dynamic component of PPG signals from a single subject that have been corrupted to varying degrees by motion artefact of a relatively high frequency (figure 3). A PPG signal with artefact measured to be 10% or under is considered to be clean and uncorrupted, whilst a signal with artefact measured around 20% is showing visible signs of corruption. With 50% or more artefact, the

the finger, which would cause physiological artefacts, or to produce movements that alter the optical field of view. Operating within these constraints, a large range of pure probe coupling artefacts can be generated. Movement distance can be controlled by the clip pressure, whilst varying the average distance between the finger and the opto-electronics simulates the effects of differing source intensity, coupling efficiency and physiological variability.

Complex movements can be generated in a multitude of ways in a clinical environment, making it impossible to perform an exhaustive analysis. In addition a large number of movements, such as the raising or lowering of the arm, will only produce physiological artefacts because they do not have a direct effect on the finger probe. The range of physical movements that can directly effect the probe can be decomposed into a number of fundamental components, which can then be independently tested. A specific complex movement can then be expressed as a combination of these fundamental components. The fundamental components that have been identified for this study are:

1. Bending the finger at the distal phalangic joint
2. Bending the finger at the mid phalangic joint
3. Waving, or pseudo-random motions of the hand

Other movements that may appear fundamental, such as bending the finger at the knuckle or exerting pressure on the probe body are not considered here because the artefacts that they produce are predominantly physiological and therefore do not fall within the scope of our definition of motion artefact. Indeed, in PPG contexts other than pulse oximetry many of these physiological dynamics may be considered valuable information^[35]. Data sets of 25 seconds in length were utilised for each class of experiment. The spectral artefact measurement was applied to both the unequalised and equalised signals for a number of data sets, resulting in pairs of values that are indicative of the artefact reduction performance. The difficulty in generating artefact of a pre-defined magnitude dictated that a number of experiments inducing artefacts of varying size were performed, with the resulting data sets being sorted and ranked according to the measured artefact. A plot of these artefact pairs can then demonstrate individual data set performance, as well as indicating trends in the performance with artefact severity.

7. RESULTS

The level of artefact reduction achieved under conditions of pure probe-coupling artefact is demonstrated in figure 4, with artefact levels of around 80% of signal power being effectively reduced to a level that is below the minimum sensitivity of the spectral artefact measure. There is no obvious trend in the artefact measure of the equalised signals with increasing artefact, suggesting a high degree of equalisation with almost zero residual artefact. This hypothesis may be confirmed by visual inspection of the data sets (see figure 1 for one example), which show near-perfect equalisation.

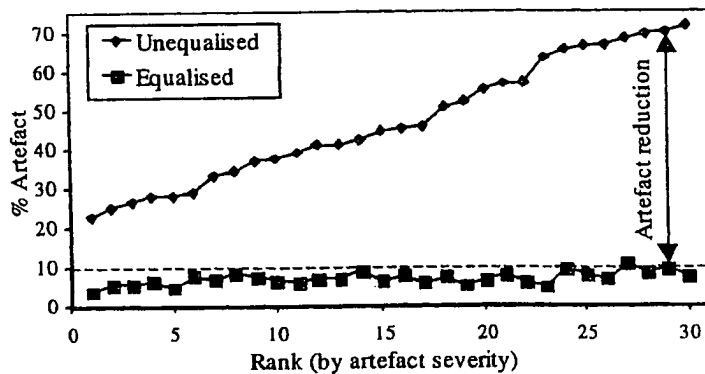


Figure 4 – Pure probe-coupling equalisation

Bending the finger at the mid phalangic joint caused artefacts that were almost completely removed by the reduction process, with some measurable residual artefact left on the equalised signal for severe artefacts in excess of about 40% of signal power. This is highlighted by the trend in residual equalised artefact with artefact severity indicated in figure 6. This suggests that while this class of movements induces artefacts that are predominantly probe-coupling in nature, more severe

Equally impressive levels of artefact reduction were achieved during periods of bending the finger at the distal phalangic joint, with artefact levels up to 90% of signal power being reduced to below the sensitivity of the measurement (see figure 5). It should be noted that the varying scales of artefact generated are indicative of the inherent maximum artefact severity that can be practically achieved with each class of experiment. This result implies that artefacts generated in this way obey the assumptions of probe-coupling artefact to a high degree, and can therefore be successfully removed using the non-linear methodology.

movements can cause additional effects, such as physiological dynamics or skewing of the probe geometry, that cannot be removed by this methodology.

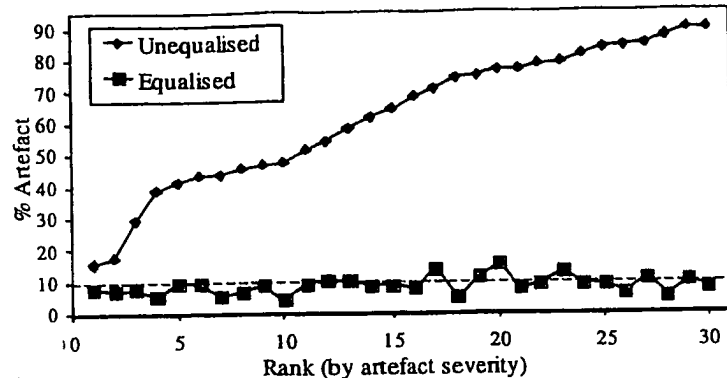


Figure 5 – Equalisation of artefact caused by bending the finger at the distal phalangic joint

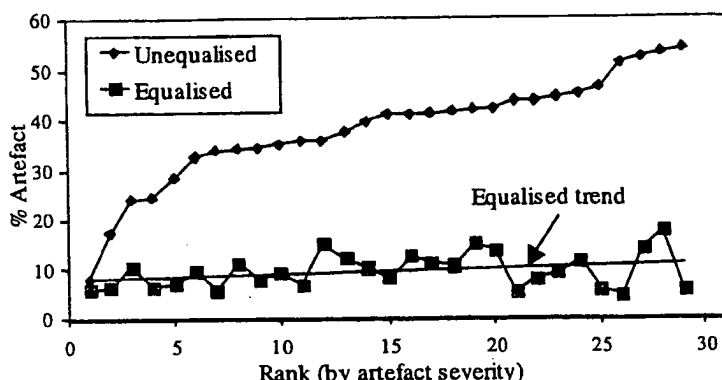


Figure 6 – Equalisation of artefact caused by bending the finger at the mid phalangic joint

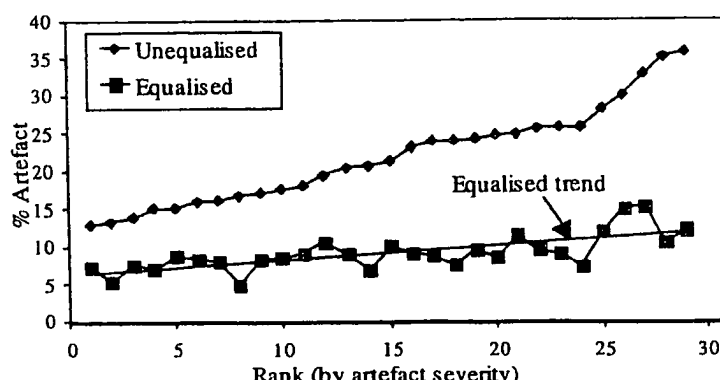


Figure 7 – Equalisation of artefact caused by pseudo-random hand movements (waving)

Waving the hand in a pseudo-random manner resulted in artefact that was reduced in all cases, with almost zero residual artefact when the movement was not severe. Severe artefacts of this class were not completely removed by this technique, again demonstrated by the trend in the equalised signal with artefact severity (see figure 7). It is likely that the geometrical skewing that can result from rapid and exaggerated hand movements is responsible for this effect. It should be noted, however, that even in cases of incomplete artefact removal there is still a significant improvement in signal quality that results from the removal of all probe-coupling effects.

The results obtained in this study demonstrate that a high degree of artefact reduction is possible with this technique in the context of transmission-mode pulse oximetry. Realistic artificial artefacts, designed to simulate practical clinical experience with finger probes, have been removed or significantly reduced by the methodology. Other effects, such as physiological dynamics or skewing of the probe geometry, result in only partial artefact reduction. It is also worth noting the performance of artefact reduction with all classes of experiment when the artefact is very mild. In these cases it may be difficult even to observe the artefact manually. The fact that the spectral artefact measure demonstrates reduction in these very mild cases highlights the presence of mild signal corruption that could cause inaccuracies in pulse oximeter output, despite the absence of an end-user perception of artefact problems.

8. DISCUSSION

It has been demonstrated that non-linear PPG artefact reduction may be applied to pulse oximetry measurement, by using a common control source to equalise both measurement signals. Several options for a suitable wavelength for the control source have been identified, depending on the measurement wavelengths utilised. The resulting formulation is not only insensitive to the effects of probe-coupling motion artefact, but represents a generalisation of the conventional formulation that introduces an extra factor into the empirical calibration process. This

methodology also results in an engineering simplification for implementation, by removing the need to consider the static signal levels in the calibration scheme.

The degree of artefact reduction achieved by this methodology has been investigated by spectral artefact quantification before and after the equalisation process. The use of a commercial transmission-mode finger-probe has allowed us to explore the effects of a number of fundamental types of motion artefact that may be encountered in a clinical environment. It has been highlighted that a significant proportion of common artefacts are predominantly probe-coupling in nature, and therefore can be effectively removed by this technique. In addition, a significant improvement of signal quality may still be observed for artefacts that are only partially probe-coupling in nature.

Whilst it is acknowledged that certain types of artefact do not conform to the probe-coupling model, and therefore cannot be removed with this technique, the simplicity of implementation implies that it could be used in conjunction with other extant signal processing solutions or artefact recognition techniques. It is also observed that the analogue and continuous nature of the technique can result in improvement of signal quality under conditions of extremely mild artefact that may not be recognised by other techniques. The effect of such mild artefact would be to reduce the accuracy of calibrated oxygen saturation output, even when the pulse rate could be determined correctly. This suggests that non-linear artefact reduction should be incorporated into conventional pulse oximetry systems, even in the absence of end-user perception of artefact problems.

9. ACKNOWLEDGEMENTS

One author (M.H.) acknowledges the financial support of both the Engineering and Physical Sciences Research Council UK and the Defence Research Agency UK.

10. REFERENCES

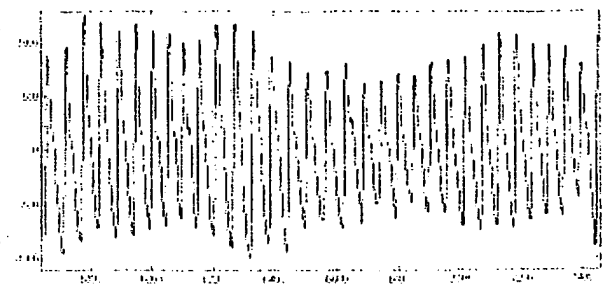
- [1] I. Yoshiya, Y. Shimada and K. Tanaka, "Spectrophotometric monitoring of arterial oxygen saturation in the finger tip", *Med. Biol. Eng. Comput.* **18**, 27-32 (1980).
- [2] W. B. Runciman, R. K. Webb, L. Barker and M. Currie, "The Pulse Oximeter: Applications and Limitations – An Analysis of 2000 Incident Reports", *Anaesth. Intensive Care* **21**, 543-550 (1993).
- [3] W. G. Zijlstra, A. Buursma and P. Meeuwsen-van der Roest, "Absorption spectra of Human Fetal and Adult Oxyhemoglobin, De-Oxyhemoglobin, Carboxyhemoglobin, and Metahemoglobin", *Clin. Chem.* **37**, 1633-1638 (1991).
- [4] A. B. Hertzman, "Photoelectric plethysmograph of the fingers and toes in man.", *Proc. Soc. Exp. Biol. Med.* **37**, 529 (1937).
- [5] N. S. Trivedi, A. F. Ghouri, N. K. Shah, E. Lai and S. J. Barker, "Effects of motion, ambient light, and hypoperfusion on pulse oximeter function", *J. Clin. Anesth.* **9**, 179-183 (1997).
- [6] M. B. Taylor and J. G. Whitwam, "The accuracy of pulse oximeters", *Anaesthesia* **43**, 229-232 (1988).
- [7] A. T. Costarino, D. A. David and T. P. Keon, "Falsely normal readings with the pulse oximeter", *Anesthesiology* **67**, 830-831 (1987).
- [8] L. H. Norton, B. Squires, N. P. Craig, G. McLeay, P. McGrath and K. I. Norton, "Accuracy of pulse oximetry during exercise stress testing", *Int. J. Sports Med.* **13**, 523-527 (1992).
- [9] R. F. Grace, "Pulse Oximetry - Gold standard or false sense of security?", *Med. J. Aust.* **160**, 638-644 (1994).
- [10] K. K. Tremper and S. J. Barker, "Pulse oximetry", *Anesthesiology* **70**, 98-108 (1989).
- [11] C. F. Poets and V. A. Stebbens, "Detection of movement artifact in recorded pulse oximeter saturation", *Eur. J. Pediatr.* **156**, 808-811 (1997).
- [12] L. Wiklund, B. Hok, K. Stahl and A. Jordetby-Jonsson, "Postanaesthesia monitoring revisited: Frequency of true and false alarms from different monitoring devices", *J. Clin. Anesth.* **6**, 182-188 (1994).
- [13] M. J. Hayes, P. R. Smith, D. M. Barnett, M. D. L. Morgan, S. Singh and D. D. Vara, "Quantitative Investigation of Artefact in Photoplethysmography and Pulse Oximetry for Respiratory Exercise Testing", in *Proceedings of the Seventh International Symposium CNVD (Computer-aided Noninvasive Vascular Diagnostics)*, V. Blažek and U. Schultz-Ehrenburg Eds. (Verein Deutscher Ingenieure, Düsseldorf, Germany, 1998) **263**, pp. 117-124.
- [14] L. Gaskin, J. Thomas, "Pulse oximetry and exercise", *Physiotherapy* **81**, 254– 61 (1995).

- [15] H. Benoit, F. Costes, L. Feasson, J. R. Lacour, F. Roche, C. Denis, A. Geyssant and J. C. Barthelemy, "Accuracy of pulse oximetry during intense exercise under severe hypoxic conditions", *Eur. J. Appl. Physiol.* **76**, 260-263 (1997).
- [16] S. J. Barker and N. K. Shah, "The effects of motion on the performance of pulse oximeters in volunteers", *Anesthesiology* **86**, 101-108 (1997).
- [17] F. E. Block, "Interference in a pulse oximeter from a fibre-optic light source", *J. Clin. Monit.* **3**, 210-211 (1987).
- [18] L. Hanowell, J. H. Eisele and D. Downs, "Ambient light affects pulse oximeters" [letter], *Anesthesiology* **67**, 864-865 (1987).
- [19] P. R. Hall, "Motion artefact rejection system for pulse oximeters", United States Patent No:4955379 (1990).
- [20] D. B. Swedlow, "Apparatus for the detection of motion transients", United States Patent No:5226417 (1993).
- [21] G. R. Matthews., "Pulse Responsive Device", International Patent Application WO 91/18550 (1991).
- [22] M. K. Diab, "Signal Processing Apparatus", International Patent Application WO 96/12435 (1996).
- [23] D. B. Swedlow, "Oximeter with Motion Detection for Alarm Modification", International Patent Application WO 94/22360 (1994).
- [24] A. R. Visram, R. D. M. Jones, M. G. Irwin and J. Bacon-Shone, "Use of two oximeters to investigate a method of movement artifact rejection using photoplethysmographic signals.", *Br. J. Anaesth.* **72**, 388-392 (1994).
- [25] K. Hamaguri and T. Sakai, "Multi-wavelength oximeter having a means for disregarding a poor signal", United States Patent No:4714341 (1987).
- [26] Stone R.T, "Method and apparatus for calculating arterial oxygen saturation based plethysmographs including transients", United States Patent No:5078136 (1992).
- [27] T. J. Yorkey, "Method and Apparatus for Removing Motion Artifact and Noise from Pulse Oximetry", International Patent Application WO 97/00041 (1997).
- [28] D. Parker, "Optical Monitor (Oximeter etc.) with Motion Artifact Suppression", International Patent Application WO 94/03102 (1994).
- [29] C. Dumas, J. A. Wahr and K. K. Tremper, "Clinical evaluation of a prototype motion artifact resistant pulse oximeter in the recovery room", *Anesth. Analg.* **83**, 269-272 (1996).
- [30] M. J. Hayes and P. R. Smith, "Artifact Reduction in Photoplethysmography", *Appl. Opt.*, at press.
- [31] J. L. Plummer, A. H. Ilsley, R. R. L. Fronsko and H. Owen, "Identification of movement artifact by the Nellcor N-200 and N-3000 pulse oximeters", *J. Clin. Monit.* **13**, 109-113 (1997).
- [32] T. Aoyagi, M. Kishi, K. Yamaguchi and S. Wantanabe, "Improvement of the ear piece oximeter", *Abstracts Jpn. Soc. Med. Electronics Biol. Engineer*, 90 - 91 (1974).
- [33] Y. Shimada, I. Yoshiya, N. Oka and K. Mamaguri, "Effects of multiple scattering and peripheral circulation on arterial oxygen saturation, measured with a pulse-type oximeter", *Med. Biol. Eng. Comput.* **22**, 475-478 (1984).
- [34] P. D. Manheimer, J. R. Casciani, M. E. Fein and S. L. Nierlich, "Wavelength selection for low-saturation pulse oximetry", *IEEE Trans. Biomed. Eng.* **44**, 148-158 (1997).
- [35] H. B. Abramowitz, L. A. Queral, W. R. Flinn, P. F. Nora, et al., "The use of photoplethysmography in the assessment of venous insufficiency: a comparison to venous pressure measurement", *Surgery* **86**, 434-441 (1979).

Photoplethysmograph

From Wikipedia, the free encyclopedia

A photoplethysmograph(PPG) is an optically obtained plethysmograph, a volumetric measurement of an organ. A PPG is often obtained by using a pulse oximeter which illuminates the skin and measures changes in light absorption (Shelley and Shelley, 2001). A conventional pulse oximeter monitors the perfusion of blood to the dermis and subcutaneous tissue of the skin.



Representative PPG taken from an ear pulse oximeter.
Variation in amplitude are from Respiratory Induced Variation.

With each cardiac cycle the heart pumps blood to the periphery. Even though this pressure pulse is somewhat damped by the time it reaches the skin, it is enough to distend the arteries and arterioles in the subcutaneous tissue. If the pulse oximeter is attached without compressing the skin, a pressure pulse can also be seen from the venous plexus, as a small secondary peak.

The change in volume caused by the pressure pulse is detected by illuminating the skin with the light from a Light Emitting Diode (LED) and then measuring the amount of light either transmitted or reflected to a photodiode. Each cardiac cycle appears as a peak, as seen in the figure. Because blood flow to the skin can be modulated by multiple other physiological systems, the PPG can also be used to monitor breathing, hypovolemia, etc.

Additionally, the shape of the PPG waveform differs from subject to subject, and varies with the location and manner in which the pulse oximeter is attached.

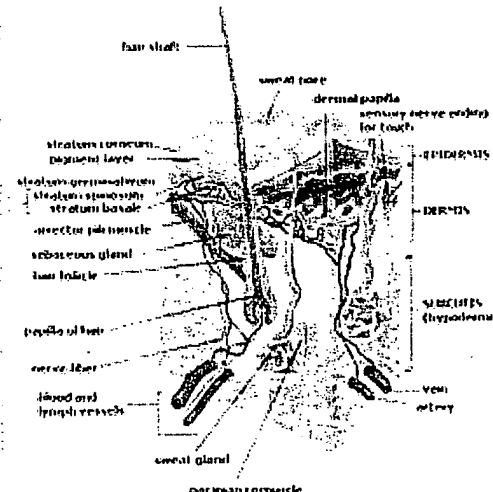


Diagram of the layers of human skin

Contents

- 1 Sites for measuring PPG
- 2 Uses
 - 2.1 Monitoring Heart Rate and Cardiac Cycle
 - 2.2 Monitoring Respiration
 - 2.3 Monitoring Depth of Anesthesia
 - 2.4 Monitoring Hypo- and Hyper-volemia
- 3 References
- 4 External links
- 5 See also

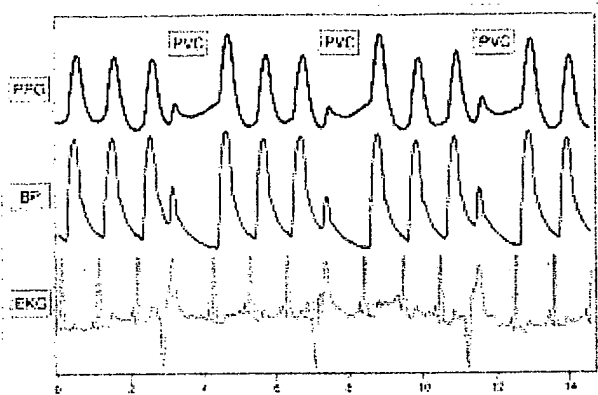
Sites for measuring PPG

While pulse oximeters are a commonly used medical device the PPG derived from them is rarely displayed, and is nominally only processed to determine heart rate. PPGs can be obtained from transmissive absorption (as at the finger tip) or reflective (as on the forehead).

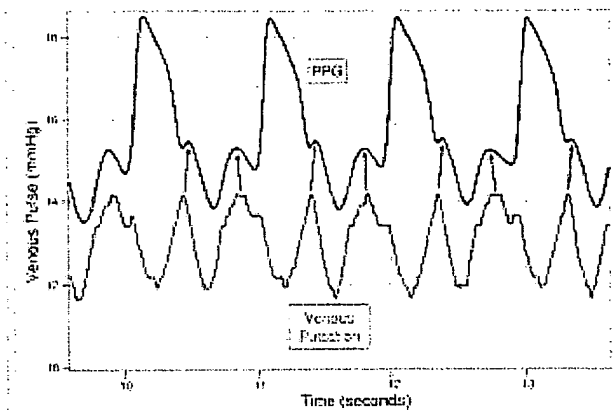
In outpatient setting pulse oximeters are commonly worn on the finger and ear. However, in cases of shock, hypothermia, etc. blood flow to the periphery can be reduced, resulting in a PPG without a discernible cardiac pulse. In this case, a PPG can be obtained from a pulse oximeter on the head, with the most common sites being the ear, nasal septum, and forehead.

PPGs can also be obtained from the vagina and esophagus.

Uses



Premature Ventricular Contraction (PVC) can be seen in the PPG just as in the EKG and the Blood Pressure (BP).



Venous pulsations can be clearly seen in this PPG.

Monitoring Heart Rate and Cardiac Cycle

Because the skin is so rich perfused, it is relative easy to detect the pulsatile component of the cardiac cycle. The DC component of the signal is attributable to the bulk absorption of the skin tissue, while the AC component is directly attributable to variation in blood volume in the skin caused by the pressure pulse of the cardiac cycle.

The height of AC component of the photoplethysmogram is proportional to the pulse pressure, the difference between the systolic and diastolic pressure in the arteries. As seen in the figure showing Premature Ventricular Contractions (PVCs) the PPG pulse for the cardiac cycle with the PVC results in lower amplitude blood pressure and a PPG. Ventricular Tachycardia and Ventricular Fibrillation can also be detected.

Monitoring Respiration

Respiration effects the cardiac cycle by varying the intrapleural pressure, the pressure between the thoracic wall and the lungs. Since the heart resides in the thoracic cavity between the lungs, the partial pressure of inhaling and exhaling greatly influence the pressure on the vena cava and the filling of the right atrium. This effect is often referred to as normal sinus arrhythmia.

During inspiration, intrapleural pressure decreases by up to 4 mm Hg which distends the right atrium, allowing for faster filling from the vena cava, increasing ventricular preload, and increasing the stroke volume. Conversely during expiration, the heart is compressed, decreasing cardiac efficiency and reducing stroke volume. However, the overall net effect of respiration is to act as pump for the cardiovascular system. When the frequency and depth of respiration increases, the venous return increase leading to increased cardiac output. (Shelley, et. al., 2006)

Monitoring Depth of Anesthesia

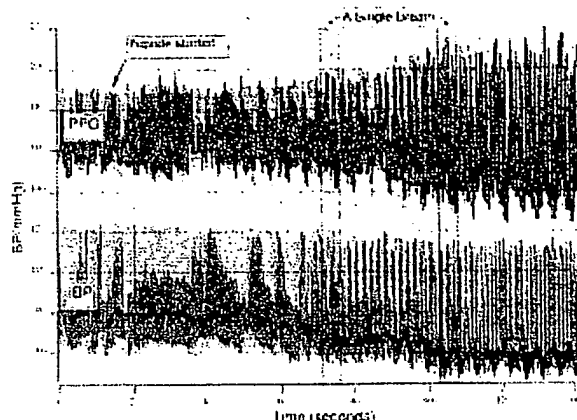
Anesthesiologist must often judge subjectively whether a patient is sufficiently anesthetized for surgery. As seen in the figure if a patient is not sufficiently anesthetized the sympathetic nervous system response to an incision can generate an immediate response in the amplitude of the PPG.

Monitoring Hypo- and Hyper-volemia

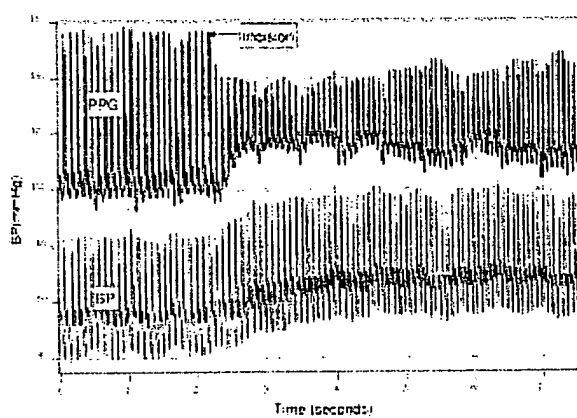
Shamir, Eidelman, et. al. studied the interaction between inspiration and removal of 10% of a patient's blood volume for blood banking before surgery(Shamir, Eidelman et al. 1999). They found that blood loss could be detected both from the photoplethysmogram from a pulse oximeter and an arterial catheter. Patients showed a decrease in the cardiac pulse amplitude caused by reduced cardiac preload during exhalation when the heart is being compressed.

References

1. M. Shamir, L. A. Eidelman, Y. Floman, L. Kaplan, and R. Pi-zov, *Pulse Oximetry Plethysmographic Waveform During Changes in Blood Volume*, Br. J. Anaesth., vol. 82, pp. 178-181, 1999.
2. K. Shelley and S. Shelley, *Pulse Oximeter Waveform: Photoelectric Plethysmography*, in Clinical Monitoring, Carol Lake, R. Hines, and C. Blitt, Eds.: W.B. Saunders Company, 2001, pp. 420-428.
3. K. H. Shelley, D. H. Jablonka, A. A. Awad, R. G. Stout, H. Rezkanna, and D. G. Silverman, *What Is the Best Site for Measuring the Effect of Ventilation on the Pulse Oximeter Waveform?* Anesth Analg, vol. 103, pp. 372-377, 2006.



The effects of Sodium Nitroprusside(Nipride) a peripheral vasodilator on the finger PPG of a sedated subject. As expected the PPG amplitude increases after infusion and additionally the Respiratory Induced Variation (RIV) becomes enhanced.



Effects of an incision on a subject under general anesthesia on the photoplethysmograph (PPG) and blood pressure (BP).

External links

A student project: building a device for collecting PPGs
(<http://www.swarthmore.edu/NatSci/echeeve1/Class/e72/E72Cardio/E72Cardio.html>)

See also

Hemodynamics

Retrieved from "<http://en.wikipedia.org/wiki/Photoplethysmograph>"

Categories: Cardiology | Medical tests

-
- This page was last modified 07:23, 15 November 2006.
 - All text is available under the terms of the GNU Free Documentation License. (See **Copyrights** for details.) Wikipedia® is a registered trademark of the Wikimedia Foundation, Inc.

Multivariate spectral analysis of the beat-to-beat sampled cortical NIRS-signals and the heart rate variability

Udo J. Scholz, Matthias Kohl, Christian Nolte, Carsten Hennig and Arno Villringer

Department of Neurology, Charite, Humboldt University, Berlin, Germany

ABSTRACT

Heart-beat-synchronous variations represent a significant noise during functional near-infrared spectroscopy (NIRS) measurements of the brain. ECG-synchronous sampling allows the heart beat correlated pulsatility to be removed from NIRS-signals. During visual stimulation the measured cortical oxy- and deoxy-hemoglobin (oxy-Hb, deoxy-Hb) responses showed a factor >2 improved signal to noise ratio (SNR) in comparison to a fixed sampling frequency.

The beat to-beat concentrations of oxy-Hb, deoxy-Hb, the redox status of cytochrome-oxydase (Cyt-Ox) as well as the heart rate variability were analysed in the frequency domain in order to find a possible correlation between the concentrations and the cardiovascular rhythms. A coherence analysis revealed a close link of these signals in the low frequency band (LF, 0.05 - 0.15 Hz) and the high frequency band (HF, 0.2 - 0.35 Hz). For the different concentration signals a different degree in coherence in the LF- and HF-bands could be observed.

Spectral analysis revealed that the cardiovascular rhythms (LF and HF) may represent a noise source in the NIRS-signals which might be removed by special digital filters.

Keywords: cortical activation, NIRS, beat-to-beat variability, coherence analysis, transfer function.

1. INTRODUCTION

The heart beat correlated pulsatility superposed on the concentrations of oxy- and deoxy-hemoglobin and the redox status of cytochrome-oxydase (oxy-Hb, deoxy-Hb, Cyt-Ox), derived by NIRS, leads to a long averaging procedure in order to obtain significant responses in cortical stimulation experiments. To overcome this problem, a high-speed sampling of the NIRS signals was proposed together with a sequential adaptive filter¹. A shorter averaging period due to a better signal to noise ratio (SNR) may be expected. Alternatively to this computational intensive procedure we suggest an ECG-synchronous sampling to obtain NIRS concentration signals without a contribution of the heart beat correlated signals. This beat-to-beat sampling allows a further multivariate analysis of the NIRS concentration signals by including the heart rate variability.

A physiological origin has been defined for the three main frequency components of the heart rate variability²:

- The 'respiratory' rhythm of heart beat variation (whose frequency is synchronous to the respiration rate), defined as high-frequency (HF) spectral component, is generally considered as a marker of vagal modulation;
- the rhythm corresponding to vasomotor waves and present in heart beat and arterial pressure (also referred to as Mayer waves) variabilities, is defined as the low-frequency (LF) component. Since it is always increased during sympathetic stimulation, it is considered to be an indicator of sympathetic activation;
- the very low frequency (VLF) component, is assumed to be due to long term regulatory mechanisms, such as humoral factors, temperature and other slow components;

Aim of this study was to investigate the relationship and interaction of cardiovascular rhythms and the NIRS concentration signals in different frequency bands (LF, 0.05 - 0.15 Hz and HF, 0.2 - 0.35 Hz) during rest and cortical activation.

¹Correspondence to uscholz@neuro.charite.hu-berlin.de; WWW: www.charite.de/ch/neuro
Telephone 0049-30-450-60006, Fax: -60938

2. METHODS

We measured the response of oxy-Hb, deoxy-Hb and Cyt-Ox over the occipital cortex to photostimulation (PS, 10 Hz checkerboard, 2s duration) in 8 normal subjects. Assuming a time-constant of the PS-responses in the range of the hemodynamic response function found in fMRI measurement ($\tau = 7\text{ s}$), a beat-to-beat acquisition of the optical signals can be performed without significant loss in information. A CCD-camera was externally triggered by a ECG-monitor which provides an on-line R-peak detection. Changes in the reflected light intensity (720 – 900 nm) were recorded by a CCD detector in combination with an imaging spectrograph and converted into changes in oxy-Hb and deoxy-Hb³.

The ECG and respiration- signal were recorded by a CED 1401 analog data acquisition system using the Spike2 software (CED, Cambridge, UK), which provided also the triggering of the photostimulus. The signals were transformed to the tachogram (R-R interval series) and the respirogram, i.e. the respiration signal sampled simultaneously to the R-peak.

An averaging procedure was applied for the analysis of the oxy-Hb, deoxy-Hb and heart rate responses to PS. The beat-to-beat signals were interpolated by a cubic spline and resampled at 4 Hz. The baseline was computed by the mean of the values ranging from 5 s to 0.5 s before stimulation onset of a set of all single responses. Significant changes due to PS were detected by comparing the baseline values to the values obtained at time t_i of the set of responses, moving t_i from stimulus onset to 30 s after onset by half-second steps. For this statistical analysis we used the t-test with $P < 0.05$. This procedure and the following signal processing was done in Matlab (Math Works, Natick, MA).

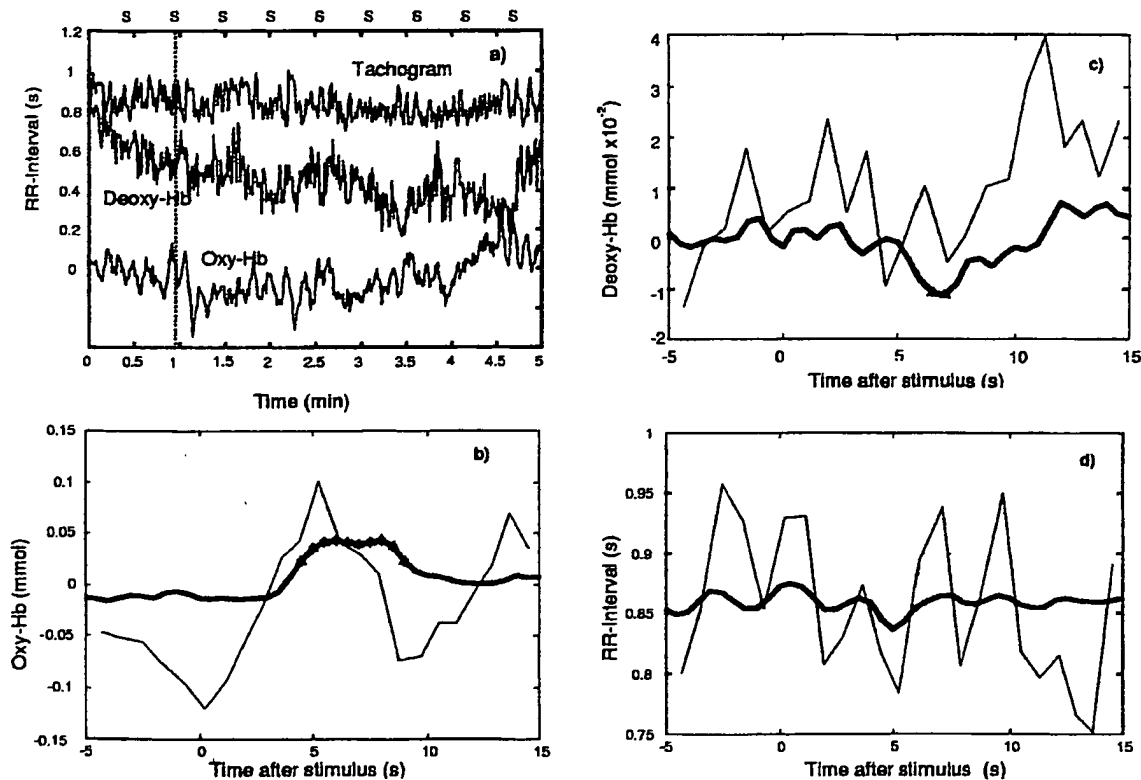


Fig 1 Time courses of a subject with a very low signal to noise ratio of the NIRS signals. a) Segment of 5 min with tachogram, deoxy-Hb and oxy-Hb concentrations. Begin of stimuli are marked by a 'S', y-axis valid for the tachogram, oxy-Hb and deoxy-Hb have arbitrary scales. Single response for stimulus $t=53.5\text{ s}$ (broken lines) and averaged responses (thick line) for b) oxy-Hb, c) deoxy-Hb and d) tachogram.

Significances: $\star P < 0.02$, $\Delta P < 0.05$.

Furthermore, an automatic spectral decomposition of the auto-spectra by residual integration and the calculation of each component power was performed⁵. The total power, its LF- and HF-component power of the tachogram, respirogram, oxy-Hb, deoxy-Hb and Cyt-Ox signals were determined. The normalized transfer function $H_{xy}(f)$ was calculated by dividing the value of the cross-spectrum $S_{xy}(f)$, by the input auto-spectrum $S_{xx}(f)$, at each frequency f and the normalized to the mean values of the input (x) and output (y) variables^{6,7} as well as the coherence function⁸.

3. RESULTS

In a comparative study with a fixed sampling frequency (50Hz) the ECG-synchronous sampling procedure an improvement of the SNR of a factor 2 was obtained. Figure 1 shows the time course a) and the averaged responses of oxy-Hb b) deoxy-Hb c) and the tachogram d) of a typical subject. A significant response to photostimulation (PS) could be observed in the NIRS-

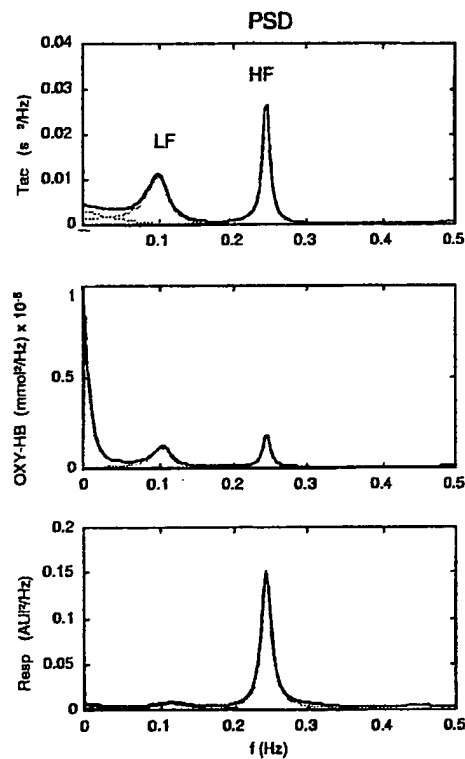


Fig. 2 Spectral analysis of the tachogram, oxy-Hb concentration and respiration. The broken lines indicate results of the automatic spectral decomposition.

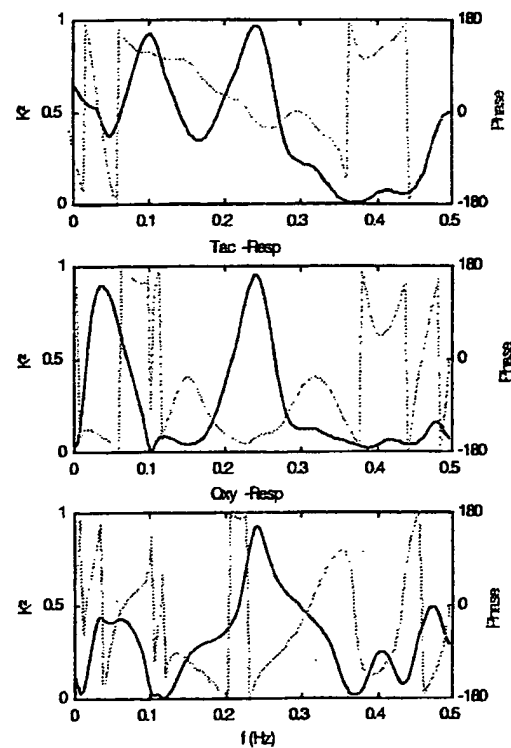


Fig. 3 Coherence plots from the same signals. Squared coherence K^2 (solid line) and phase (broken line).

The spectral analysis (Fig. 2) showed a LF- and HF-activity in oxy-Hb signal, with approximately 30% of total signal power. The bivariate spectral analysis of the same subject (Fig 3) which was calculated on couples of the oxy-Hb with the tachogram and respirogram established the squared coherence K^2 in each frequency range. Values of K^2 close to 1 confirms that the specific rhythm is related to a common source or that a close link between the signals exists. Figure 3 shows, that a significant coherence K^2 was obtained in the LF and HF bands for the oxy-Hb signal and the tachogram as well as a high K^2 in the HF band only in the case of the respirogram. No significant changes could be found between the periods without PS of 3 min duration and the period with stimulation.

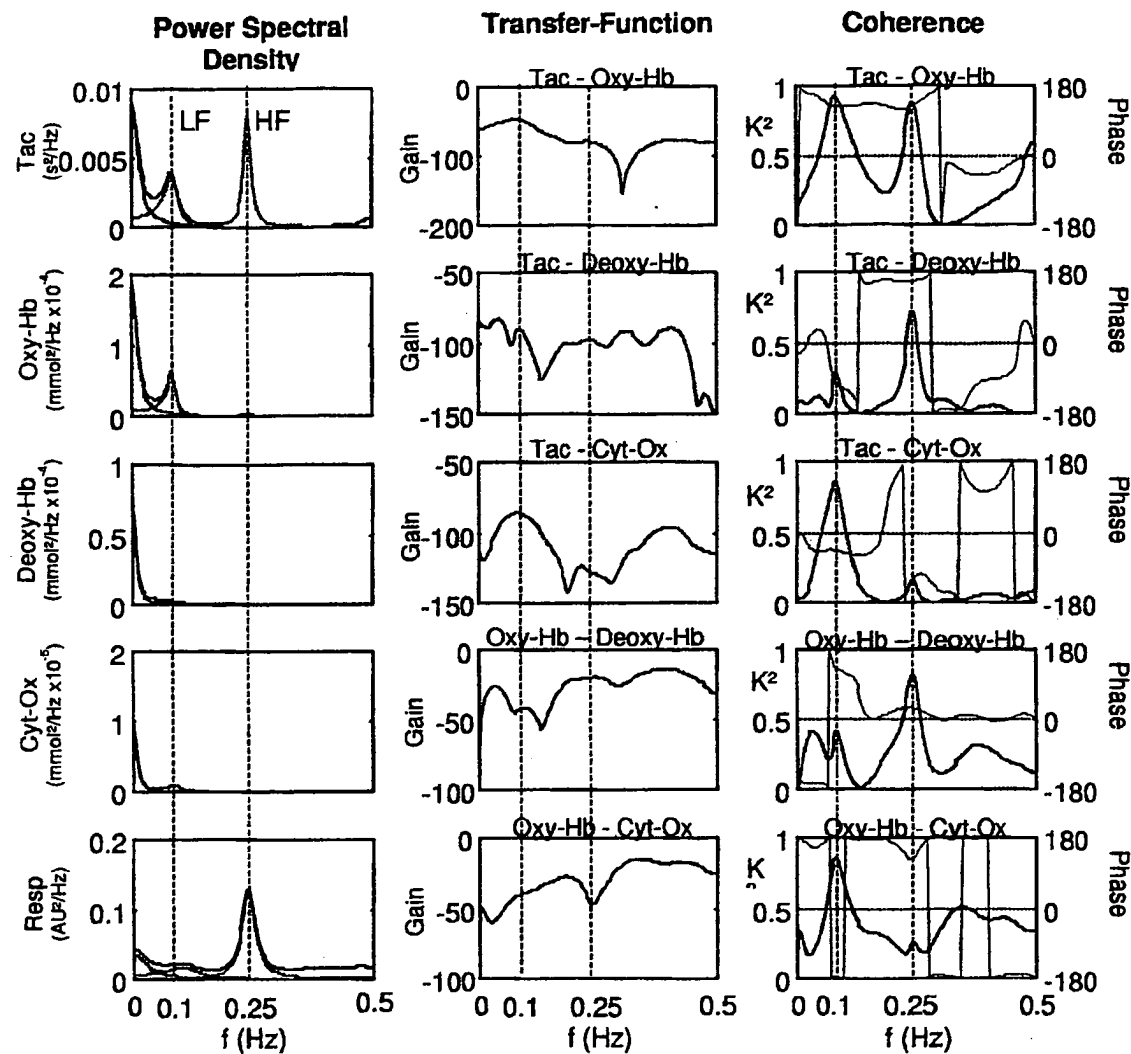


Fig. 4 Multivariate spectral analysis of tachogram (TAC), NIRS signals (oxy-Hb, deoxy-Hb, Cyt-Ox) and Respiration (Resp). Autospectrum (P_{xx} , left), gain of transfer function ($20 \log |H_{xy}|$, middle), coherence function (K^2 , right, solid line) and phase (right, broken line). The vertical broken lines indicate the center frequencies of the LF and HF components.

Figure 4 shows the results of the multichannel analysis including the transfer functions. A negative gain indicates that the output varies less than the input and a positive value indicates that the output varies greater than the input. In the transfer function Tac-oxy, that describes how the input Tachogram affects the output oxy-Hb, the gain showed the largest value in the LF-band and decreasing continuously until 0.3 Hz, describing a low-pass filter with an upper frequency edge at the upper end of the HF-band. In the gain over frequency plots of the other concentration signals notches in the course may be observed: in the LF-band in the case of the output deoxy-Hb and in the HF-band for the Cyt-Ox signal. This leads also to significant differences in the coherence plot for that signals: a low K^2 in the LF-band and a high one in the HF-band for the deoxy-Hb and vice versa for the Cyt-Ox signal.

4. DISCUSSION

In this study cortical NIRS measurements during visual stimulation of 8 healthy subjects were analysed. The ECG-synchronous sampling allowed the heart beat correlated pulsatility to be removed from NIRS-signals.

A signal to noise ratio (SNR) improved by a factor >2 in comparison to a fixed sampling frequency. This is a similar improvement as reported by studies involving a high speed sampling and a least-squares regression algorithm for compensating of the artifact introduced by the pulse (factor 2.1)¹. Due to the increased SNR, the beat-to-beat sampling allowed a reduction of the number of stimuli necessary for a significant response during stimulation experiments.

The coherence analysis confirmed that oscillations (LF- and HF-rhythm) of cardiovascular origin are present in the NIRS concentration signals. In this study the oxy-Hb, deoxy-Hb and Cyt-Ox response to the oscillations in the heart rate variability was investigated by a transfer function analysis. A different behavior of that response to LF- and HF-rhythms was evident for the different concentrations.

The result was that cortical activation due to visual stimulation did not change the general characteristics of the transfer functions and coherence plots compared to rest condition. The expected lack of response to visual stimulation on heart rate (Fig 1d) indicated that no autonomic changes were evoked and no relevant dynamics in cerebral autoregulation was induced by the visual stimulation. Further experiments including cardiovascular reflex test are probably needed to investigate the observed phenomena in more detail.

The cardiovascular rhythms (LF and HF) represent another noise source in the NIRS-signals with up to 30% of the total signal power. To remove this rhythms a digital notch filter, similar to those established in functional MRI⁹ may be constructed with 2 frequencies centered at the LF- and HF-rhythms, as identified by the spectral analysis.

In the future a multivariate analysis will be extended to other beat-to-beat cerebro- and cardiovascular variability signals like blood pressure or cerebral blood flow velocity as measured by transcranial Doppler sonography. This technique may help to quantify the neurovascular coupling during different states of autonomic and cortical activation. In this study no definite answer to the physiological meaning of these rhythms in the NIRS concentration signal was given.

5. REFERENCES

1. G. Gratton and P.M. Corballis, "Removing the heart from the brain: compensation for the pulse artifact in the photon migration signal" *Psychophysiology* 32, pp. 292-299, 1995.
2. "Heart rate variability: standards of measurement, physiological interpretation and clinical use. Task Force of the European Society of Cardiology and the North American Society of Pacing and Electrophysiology" *Circulation* 93, pp. 1043-1065, 1996.
3. M. Kohl, C. Nolte, H.R. Heekeren, S. Horst, U.J. Scholz, H. Obrig, and A. Villringer, "Determination of wavelength dependence of the differential pathlength factor from near-infrared pulse signals" *Phys.Med.Biol.* 43, pp. 1771-1782, 1998.
4. A. Neumaier and T. Schneider, "Multivariate autoregressive and Ornstein-Uhlenbeck processes: Estimates for Order, Parameters, Spectral Information, and Confidence Regions." *ACM Trans.Math.Softw.*, 1998.

5. G. Baselli, S. Cerutti, S. Civardi, F. Lombardi, A. Malliani, M. Merri, M. Pagani, and G. Rizzo, "Heart rate variability signal processing: a quantitative approach as an aid to diagnosis in cardiovascular pathologies" *Int.J Biomed.Comput.* **20**, pp. 51-70, 1987.
6. M. Pagani, V. Somers, R. Furlan, S. Dell'Orto, J. Conway, G. Baselli, S. Cerutti, P. Sleight, and A. Malliani, "Changes in autonomic regulation induced by physical training in mild hypertension" *Hypertension* **12**, pp. 600-610, 1988.
7. A.P. Blaber, R.L. Bondar, F. Stein, P.T. Dunphy, P. Moradshahi, M.S. Kassam, and R. Freeman, "Transfer function analysis of cerebral autoregulation dynamics in autonomic failure patients." *Stroke* **28**, pp. 1686-1692, Sep, 1997.
8. S.L. Marple, Jr. "Digital spectral analysis", Englewood Cliffs, NJ: Prentice Hall, 1987.
9. B. Biswal, A.E. DeYoe, and J.S. Hyde, "Reduction of physiological fluctuations in fMRI using digital filters" *Magn.Reson.Med.* **35**, pp. 107-113, 1996.

To Print: Click your browser's PRINT button.

NOTE: To view the article with Web enhancements, go to:

<http://www.medscape.com/medline/abstract>

Detection of dicrotic notch in arterial pressure signals.

J Clin Monit. 1997; 13(5):309-16 (ISSN: 0748-1977)

Hoeksel SA ; Jansen JR ; Blom JA ; Schreuder JJ

Department of Anesthesiology, Cardiovascular Research Institute Maastricht, Maastricht University, The Netherlands.

OBJECTIVE: A novel algorithm to detect the dicrotic notch in arterial pressure signals is proposed. Its performance is evaluated using both aortic and radial artery pressure signals, and its robustness to variations in design parameters is investigated. **METHODS:** Most previously published dicrotic notch detection algorithms scan the arterial pressure waveform for the characteristic pressure change that is associated with the dicrotic notch. Aortic valves, however, are closed by the backwards motion of aortic blood volume. We developed an algorithm that uses arterial flow to detect the dicrotic notch in arterial pressure waveforms. Arterial flow is calculated from arterial pressure using simulation results with a three-element windkessel model. Aortic valve closure is detected after the systolic upstroke and at the minimum of the first negative dip in the calculated flow signal. **RESULTS:** In 7 dogs ejection times were derived from a calculated aortic flow signal and from simultaneously measured aortic flow probe data. A total of 86 beats was analyzed; the difference in ejection times was -0.6 ± 5.4 ms (means \pm SD). The algorithm was further evaluated using 6 second epochs of radial artery pressure data measured in 50 patients. Model simulations were carried out using both a linear windkessel model and a pressure and age dependent nonlinear windkessel model. Visual inspection by an experienced clinician confirmed that the algorithm correctly identified the dicrotic notch in 98% (49 of 50) of the patients using the linear model, and 96% (48 of 50) of the patients using the nonlinear model. The position of the dicrotic notch appeared to be less sensitive to variations in algorithm's design parameters when a nonlinear windkessel model was used. **CONCLUSIONS:** The detection of the dicrotic notch in arterial pressure signals is facilitated by first calculating the arterial flow waveform from arterial pressure and a model of arterial afterload. The method is robust and reduces the problem of detecting a dubious point in a decreasing pressure signal to the detection of a well-defined minimum in a derived signal.

PreMedline Identifier: 9338845

Noninvasive monitoring of arterial blood oxygenation
with spectrophotometric technique

Anna Cysewska-Sobusiak

Institute of Electronics and Communications
Technical University of Poznań,
Piotrowo 3a, PL-60-965 Poznań, Poland

ABSTRACT

The spectrophotometric technique used in pulse oximetry makes it possible to determine noninvasively and continuously the oxygen saturation of arterial blood. This technique utilizes a set of the living blood-supplied tissues as an object to be measured. From the metrological point of view, the sensing efficiency, spectrophotometric processing quality, and object modelling are of great importance in reliable solution of the specific interdisciplinary problems. In this paper the main results of the author's studies concerning the optical part of measuring system have been described against a background of the reviewed generally valid principles.

1. INTRODUCTION

The advantages of the newest kind of oximetry, so-called pulse oximetry, make it one of the most significant advance made in patients monitoring^{5,6}. The noninvasive spectrophotometric technique utilizes the optical properties of the body living tissues as an object. The specific processing of the signals is unique in that it can distinguish the absorption properties of the oxygenated arterial blood from venous blood and other tissues^{7,9}. The oxygen saturation of hemoglobin $SaO_{2\%}$ is a basic parameter to be determined, however, because of the arterial pulsations which modulate the amount of light absorbed by the object, the pulse rate and waveform can be observed too.

$SaO_{2\%}$ is a one of the principal parameters of interest in hospital practice, e.g. in monitoring of the adult and infant patients during anesthesia, intensive care, and any situation in which the patient is at risk of hypoxia. Death or cerebral damage can result from undetected it. Pulse oximeters since 1990 have been recommended by the American Society of Anesthesiology as standard equipment in anesthesia practice. In many a country of East Europe these devices are not widespread, and then the traditional, risky, invasive procedures are in use by necessity. The authoress of the presented paper has been undertaken this theme. The research and experimental works are realized^{13,15}.

To use the pulse oximetry in continuous monitoring of oxygenation it is necessary to know its accuracy and to be aware of its some limitations. Especially, the measurement reliability very depends on the processing quality in the optical part of the measuring system. In this part the selective light action on the blood-supplied tissues must be realized effectively but also without destructive effects. The spectrophotometric interaction between optical radiation of the specific parameters and the chosen body site may be used in the transmissive or reflective mode. First of them, that is considered herein, usually is more sensitive^{3,12}.

2. GENERAL PRINCIPLES OF MEASUREMENTS

Definition of the functional oxygen saturation is based on assumption that hemoglobin exists in blood as the oxyhemoglobin HbO_2 and reduced hemoglobin Hb. Thus, the percentage value of this quantity can be written as :⁹

$$\text{SaO}_{2\%} = \frac{\text{HbO}_2}{\text{HbO}_2 + \text{Hb}} \cdot 100\% \quad (1)$$

Traditional spectrophotometric measurements of $\text{SaO}_{2\%}$ use the drawing samples of arterial blood. This invasive procedure only provides the intermittent informations and includes complications, such as hematomas and infection impendences. With pulse oximetry measurements are rapid, bloodless, convenient, and safe for patients. The utilized physical and physiological phenomenons are given below :

- 1/ the noninvasive selective light action on the living tissues,
- 2/ the detectable differences in light absorption spectra of HbO_2 and Hb,
- 3/ the Lambert-Beer-Bouguer's laws,
- 4/ the periodic, pulsatile presence of oxygenated blood in the arterial vessels, according to each heart beat.

With the transmissive mode, the $\text{SaO}_{2\%}$ is measured from the peripheral body sites, such as the finger-tip, ear-lobe, or nasal-bridge. With the reflective mode, the more centrally located parts can be used, such as the forehead, chest, or back. Both modes need to apply the special sensor which is setting directly to the chosen location. The transmissive mode is often more suitable and convenient^{11,12}, and the finger-tip is a best site in most of the clinical situations. Fig.1 illustrates the general block diagram of the pulse oximeter system idea.

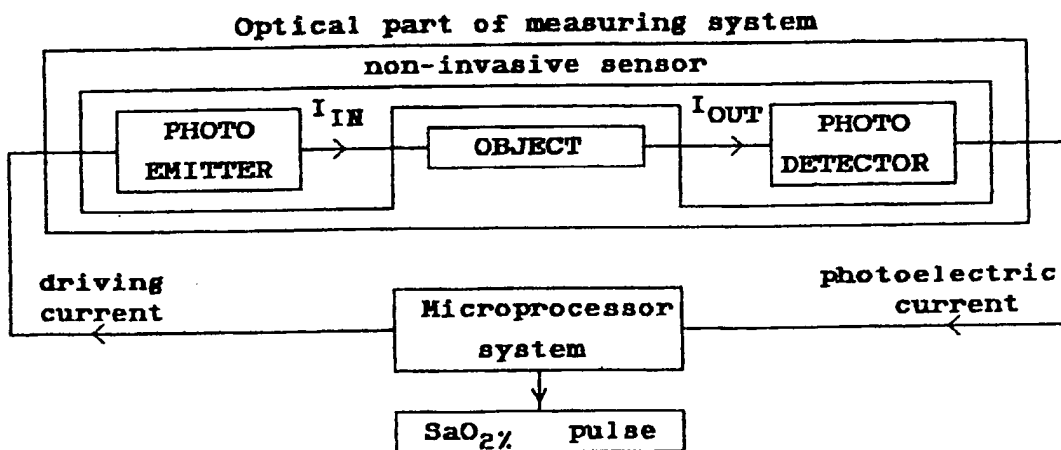


Fig.1. The block diagram of the pulse oximeter system idea in the transmissive mode

In the structure of the microprocessor-based system the optical also electronical processing is accomplished. The system design must satisfy a lot of requirements : the functional sensor is indispensable, the emitter of the input optical signals must be properly driven, and the output signals components from the photodetector must be properly amplified, separated, and filtered.

In accordance with the absorption laws, two wavelengths of light would be produced by photoemitter in order to distinguish two contents. Pulsatile changes of arterial volume make the photoplethysmographic curve which corresponds to the pulse waveform⁷. Thus, at each of wavelengths, the time-varying light transmitted by the object includes a quasi-constant level and a slowly varying pulsatile weak signal of the frequency range from tenth to several Hz. The extreme values of the pulsatile components contain the wanted information of the oxygen saturation. Dividing these amplitudes by the constant levels, and using the experimentally verified algorithm, the calibration function may be established. As a result, the $\text{SaO}_2\%$ values are estimated with the given accuracy.

The artifacts, noises, and other disturbances can delimit the reliability of measurements. The different influences concerning the microprocessor-based part of system may be reduced or eliminated by technical modifications. The following concerns the problems with the optical part of system which consists of the object and non-invasive sensor. The measurement reliability very depends on its characteristics.

3. OPTICAL PART OF MEASURING SYSTEM

3.1. Characteristics of object

The object to be measured is a complex physiological and physical structure. Figs.2 and 3 illustrate its specificity. Transillumination of that greatly attenuating medium is rich in complications, however, it may effectively be realized. Within whole object only the peripheral arterial vessels are pulsating, and then cause the cyclical change in the object volume. In the considered one-dimensional structure,

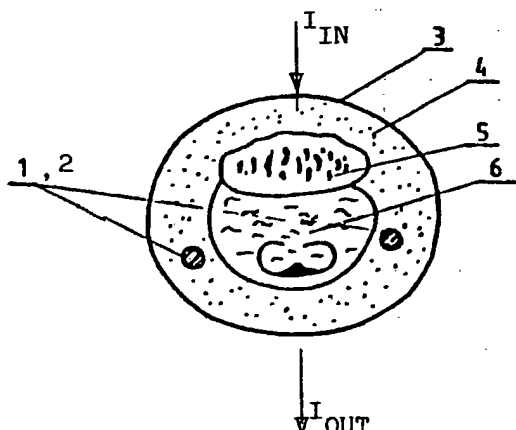


Fig.2. Physiological components of exemplary object - the finger nail phalanx is shown in the cross-section:
1,2 - arterioles, 3 - skin,
4 - vascularized and innervated subcutaneous tissue, 5 - bone,
6 - muscle tissue

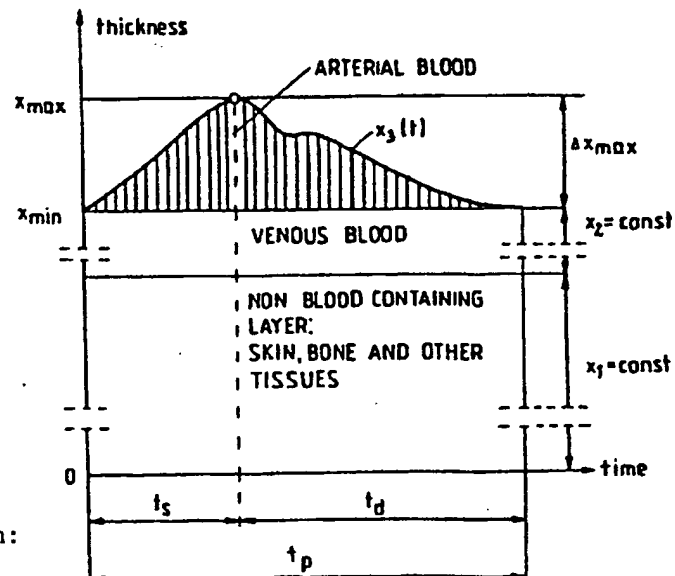


Fig.3. Constant and pulsatile components of a light path through the given object:
 $x(t)$ - thickness of the object corresponding to varying light path

the length of the light path and amount of light to be transmitted by the object are modulated. At any moment, the instantaneous value of the output light intensity $I_{OUT}(t)$ corresponds to the instantaneous value of $x(t)$. Generally, we can write :

$$x(t) = x_1 + x_2 + x_3(t) = x_{min} + \Delta x(t) \quad \dots \quad \text{the time-varying light path},$$

$$I_{OUT}(t) = I_{OUTmax} - \Delta I_{OUT}(t) \quad \dots \quad \begin{array}{l} \text{intensity of output light trans-} \\ \text{mitted by the object which depends} \\ \text{on size of the arterial pulse} \end{array}$$

change, the wavelength of the incident light intensity I_{IN} , the individual structure of tissues, and the value of SaO_2 .

As an instance, for the regular cardiac cycle, the systole and diastole phases correspond to $t_s = 1/3 \cdot t_p$ and $t_d = 2/3 \cdot t_p$. At the pulse rate from 20 to 240b.p.m. the period of pulsations p is respectively equal to $t_p = (3,00 \div 0,25)s$. For the given object, at each of two wavelengths, two extreme values of $x(t)$ and $I_{OUT}(t)$ are specific and important from the metrological point of view. The following relationships formulate these extreme events :

the background values at $t = k \cdot t_p$:

$$x(t) = x_{min}, \quad I_{OUT}(t) = I_{OUTmax} \lambda_1 \quad \text{or} \quad I_{OUTmax} \lambda_2 \quad (2)$$

the peak values at $t = k+1/3 \cdot t_p$:

$$x(t) = x_{max}, \quad I_{OUT}(t) = I_{OUTmin} \lambda_1 \quad \text{or} \quad I_{OUTmin} \lambda_2 \quad , \text{ where : } k = 0,1,\dots \\ \lambda_1, \lambda_2 - \text{measuring wavelengths.}$$

The differences between the background and peak values are equal to :

$$\Delta x_{max} = x_{max} - x_{min} \quad \text{and} \quad I_{OUTmax} - I_{OUTmin} = \Delta I_{OUTmax} \quad (3)$$

Basing on the average ratio of arterial blood and all tissues², in the real object, the value of Δx_{max} is found to be about $0,012 \cdot x_{max}$.

Theoretically, for the layer of the hemolyzed blood, it is true that :

$\Delta x = \Delta x(HbO_2) + \Delta x(Hb)$. The definition (1) and the laws of absorption are valid exactly. For the whole nonhemolyzed blood within object the situation is different because of the more composed nature of the light propagation. In the optical aspect, the object makes a set of the particulate suspensions consisting of the absorbing as well as scattering centers^{1,4}. Propagation of light is influenced by the following factors :

- 1/ absorption of light by the hemoglobin species and other pigmented particules,
 - 2/ scattering of light by the blood cells,
 - 3/ scattering of light by the non-pigmented particules in tissues.
- The physical phenomena occurring in the transilluminated object can be described by the contributions to the total transmittance T_t or total optical density OD_t . The relations between them, if to assume the object as a set of n components, are given below :

$$T_t = \frac{I_{OUT}}{I_{IN}} = \prod_{i=1}^n T_i \quad (4)$$

$$OD_t = \log \frac{1}{T_t} = \sum_{i=1}^n OD_i$$

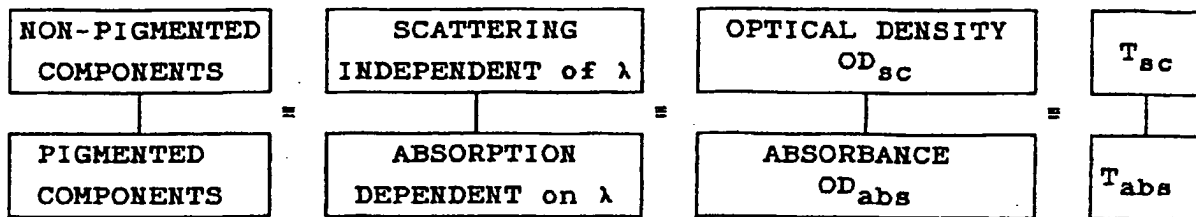


Fig.4. Contribution of the object components to the light propagation

$$OD_t = \log i / T_t = OD_{sc} + OD_{abs} ; T_t = T_{sc} \cdot T_{abs}$$

$$OD_{sc} = f(x) ; \quad OD_{abs} = \sum A = f(x, \lambda, SaO_2\%)$$

Fig.4 shows how the absorbing and scattering components of the object contribute to the final light propagation. It was assumed that^{2,4,8,12} :

- 1/ The losses of light within object, and then the decrease in transmittance, occur as a result of the multiple scattering and selective absorption.
- 2/ The scattering and absorbing centers are small compared with the object thickness.
- 3/ All the tissues significantly attenuate the optical radiation at all wavelengths. However, to take the values of λ_1 and λ_2 in the range extending from red to infrared region is only advisable for the reasons :
 - HbO_2 as well as Hb have a moderate absorption compared with that at the shorter waves,
 - non-pigmented tissues have scattering dominating over the absorption but it is independent of λ because the sizes of the scattering particles exceed it,
 - the blood cells have scattering independent of λ for the same reason also independent of the oxygen saturation.

Every layer in the object structure contributes to the scattering (OD_{sc}) or/and absorbing (OD_{abs}) parts of the total optical density.

Summarized comment

For the i -th true absorber of c_i concentration, its optical density is equal to an absorbance A_i which can be expressed as $A_i = E_i \cdot c_i \cdot x_i$, where E_i is a wavelength-dependent extinction coefficient.

For the set of absorbers, all the components of the total absorbance are additive at $\lambda = \text{const}$. The idealized relationship (1) can be written in the general form :

$$SaO_2\% = F_1 \left[\frac{\left(A_{HbO_2} + A_{Hb} \right) \lambda_1}{\left(A_{HbO_2} + A_{Hb} \right) \lambda_2} \right] \cdot 100\% \quad (5)$$

In the real object the absorption laws are valid not exactly. However, the measurements may be based on the function concerning the extreme values of the output light intensity I_{OUT} ^{7,10}. In a general way, this function can be described as :

$$SpO_{2\%} = F_2 \left[\left(\frac{\Delta I_{OUTmax}}{I_{OUTmax}} \right)_{\lambda_1} : \left(\frac{\Delta I_{OUTmax}}{I_{OUTmax}} \right)_{\lambda_2} \right] . 100\% \quad (6)$$

Value of $SpO_{2\%}$ corresponds to the pulse oximeter reading which estimates the wanted value of $SaO_{2\%}$ with a specified accuracy. The processing function (6) is experimentally established, and then is independent of the incident light intensity I_{IN} also eliminates influence of the optical densities concerning the venous blood and other non-pulsatile components of the object structure.

3.2. Metrological properties of non-invasive sensor

3.2.1. General requirements

Photoemitter and photodetector are the integral parts of the sensor. In the considered herein the transmissive mode, these parts are mounted in opposition (Fig.5).

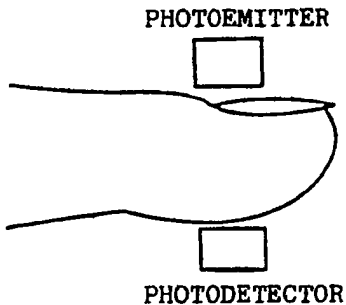


Fig.5. Configuration of the optical part of the measuring system :
 - finger-tip as a transilluminated object,
 - photoemitter and photodetector which are the integral parts of the sensor

In order to make sure an ability to function with adequate reliability of the spectrophotometric processing, the following requirements would above all be satisfied :
 1/ the convenient, easy to apply, and safe for patient sensor design,
 2/ the light action on the object with the proper values of λ_1 and λ_2 ,
 3/ high emission efficiency of the photoemitter,
 4/ high sensitivity and the low noise level of the photodetector.

All the elements of the optical part have to co-operate in the various measurement situations. Virtually, it is impossible to realize the all-purpose sensor, suitable for any objects. Different patient activity, desirable duration of monitoring, and the different sizes of objects require to select a best kind of the design. Obviously, any non-invasive sensor would always be non-aggressive for the delicate living tissues. Currently, two main kinds of design are available : hard durable and flexible adhesive.

The durable, massive, mostly plastic sensors like clips or clamps, often with the soft bed inside, are used as a standard equipment with the manufactured pulse oximeters. These sensors are setting on the finger-tips and usually positioned so that photoemitter is located at the base of the nail.

The flexible adhesive sensors, mostly like bandages or plasters, may be reusable as well as disposable. These sensors are taped on the chosen locations and especially are useful for application on infants. In this case a best body location may be object which is easy for use, such as palm or foot.

3.2.2. Measuring wavelengths

Pulse oximeter system separates the absorption properties of the arterial blood from the optical properties of all tissues. Therefore, in the selection of the measuring wavelengths the absorption spectra of blood species are decisive. Fig.6 shows the absorption curves of the detected hemoglobin species⁷. Extinction coefficient E is the light absorption of a unit concentration and light pathway of the HbO_2 and Hb respectively, on a logarithmic scale. The wavelength range extends from the blue light in the visible region up to the infrared. In this range, the wavelengths at approximately $\lambda_1 = 660\text{nm}$ and $\lambda_2 = 940\text{nm}$ are best to use for the following reasons:

- 1/ The relatively low absorbances of whole blood provide the measurable values of the light intensity to be transmitted out by the object.
- 2/ For best measurement sensitivity, two wavelengths would be such that at the λ_2 the absorption curves of HbO_2 and Hb are different as possible from their positions at the λ_1 . If to satisfy this requirement, then it is possible to obtain the detectable changes in the ratio values given in equation (6) , even for the small changes in $\text{SaO}_2\%$.
- 3/ At wavelength approximately 660nm, the difference between the HbO_2 and Hb extinction is large. Thus, at $\lambda_1 = 660\text{nm}$ the resolution of the saturation measurement may be highest.
- 4/ The absorption curves have an isobestic point at 805nm in which they cross. This point and wavelengths near it are useless in measurements because to take any of them as λ_2 could significantly reduce the measurement accuracy.
- 5/ In region from 900 to 950 nm the curves are again clearly separated. Besides, their position is inverted one another compared with that in the red region.
- 6/ In the range from 660 to 940nm the scattering of blood cells and other tissues is independent of the wavelength.

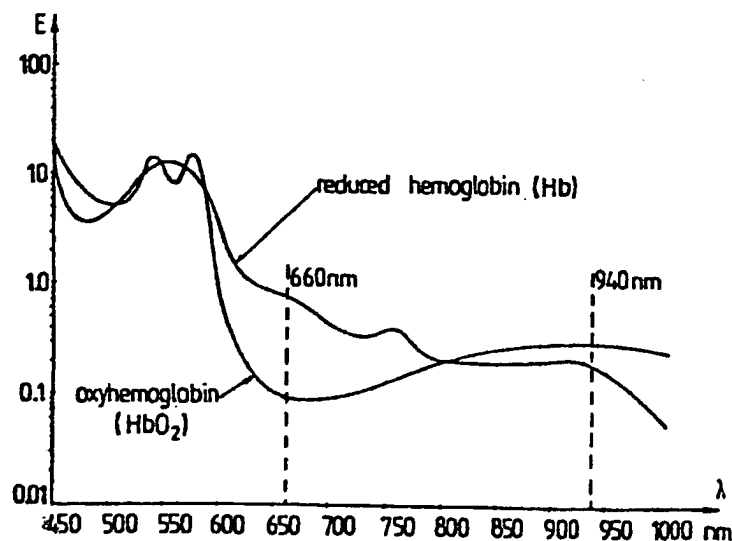


Fig.6. Absorption spectra of oxyhemoglobin and reduced hemoglobin

3.2.3. Photoemitter

The incident light must be able to penetrate the turbid and pigmented medium. Extremely bright Light Emitting Diodes (LEDs) with the plastic, uncoloured and clear lenses are favoured as photoemitters because of their special advantages which are as follows :

- 1/ LEDs are small, lightweight, durable, stable, and cheap.
- 2/ LEDs of an optical high efficiency which generate very little heat, are produced at 660nm as well as 940nm.
- 3/ The half-power bandwidth being from 20 to 30nm is satisfactory and it has no effect on the accuracy of the oxygen saturation measurement.
- 4/ The changes in the junction temperature are of moderate importance. The increase in temperature typically results in the center wavelength increase which is equal to about 0,5nm/°C.
- 5/ The dynamic properties of LEDs are determined by the rise and fall time which is equal to 10 - 20ns at 660nm, and 1 - 2μs at 940nm.

Below, the parameters for the exemplary LEDs are given :

R LED type RTL53 :

center wavelength	:	660nm
diameter of emitting area	:	5mm
brightness at the driving current 20mA	:	500mcd

IR LED type TSUS5402 :

center wavelength	:	940nm
diameter of emitting area	:	5mm
output optical power at the driving current 100mA	:	15mW

Taking into account the satisfactory dynamic properties of LEDs and that the brightness (in red region) or output power (in infrared region) of LEDs varies linearly with the driving current, there are useful practical features from the point of view of the most effective transillumination of object.

First, to drive the LEDs alternately, in the pulse mode, allows to obtain the higher intensity, without any destructive effects, and with low power consumption.

Second, to control and, if necessary, to adjust the intensity of light emitted by the given LED, according to the optical density of object, allows to provide the proper levels of light for the objects being thick and darkly pigmented as well as thin and lightly pigmented.

3.2.4. Photodetector

The output light has a very low intensity. Besides, the pulsatile components usually only little contribute to total transmittance. For example, during transillumination of the average finger-tip, the total transmittance was found to be $T_t < 0,03^{13}$. Pulsatile components of the resulting signals are no greater than from 1 to 5% of the background values. The photodetector must be able to convert the received light into electrical signal. Therefore, its high sensitivity at the considered wavelength is essential criterion what type to select. The silicon PIN photodiodes are the most suitable from this point of view. Some of their advantages which decide of utility

in sensor design, are summarized below :

- 1/ The available PIN photodiodes in the clear plastic thin packages are small, light-weight, durable, and cheap.
- 2/ High performances can be achieved at a relatively low value of reverse bias, e.g. -10V. Also, photodiodes can operate with photovoltaic effect.
- 3/ Sensitivity and stability are satisfactory over the spectrum range including the measuring wavelengths. The dark current is low and the noise equivalent power is lower than that of other kinds of photodetectors.
- 4/ The response time may be less than 1ns. The short light pulses can be detected.

Below the parameters for the exemplary PIN photodiode are given :

Type BPW34 : spectral sensitivity S_λ : 0,6A/W at $\lambda = 870\text{nm}$
half-power bandwidth $\lambda_{0,5}$: (530-1050)nm
photosensitive area : 7,5mm²
response time : 100ns

Because of the low changes in the light intensity reaching the photosensitive area, PIN photodiodes require to co-operate with the high performance amplifier system.

3.3. Factors affecting measurement reliability

The disturbances caused by each of the optical part components can decide the resultant processing reliability. Especially, there are some difficulties with sensing and processing when the disturbances are at frequencies within the physiological ranges. Generally, the factors which can interfere with an accuracy of measurements can arise from :

- 1/ Any disturbances that cause the rhythmical or irregular changes in the pulsatile component of the distance between the photoemitter and photodetector, and/or in the pulsatile component of the output light intensity.
 - 2/ Any disturbances which can vary the size of the constant background component of the optical density, and/or the constant component of the output light intensity.
- All these factors, singly or together, can result in :
- an inability to function as a consequence of inadequate pulse detection,
 - the falsely low or high values of $\text{SpO}_2\%$ compared with the $\text{SaO}_2\%$,
 - a lack of stability of the obtained output signals for the given object.

The different affecting factors respectively concern the physics and physiology of object, sensor design and application, and extraneous influences. Main of them are classified below.

3.3.1. Object physics and physiology

- 1/ Very low values of oxygen saturation, i.e. $\text{SaO}_2\% < 50\%$.
- 2/ Reasons which reduce the arterial pulsation amplitudes, such as hypothermia, hypotension, pulseless, and administration of vasoconstrictor drugs.
- 3/ Object motion and unsteady position, e.g. patient shivering and coughing.
- 4/ Abnormal structure of object, e.g. very thin or very thick tissue layer at which the transillumination procedure is resultless.
- 5/ Irregular pulse waveform and abnormal hemodynamic conditions.
- 6/ Non-pulsatile extracorporeal circulation.
- 7/ Additional absorbers in venous blood, or tissues, e.g. intravenously administered dyes, dark skin pigmentation, nail polish.
- 8/ Additional absorbers in arterial blood.

Because pulse oximeter system uses only two wavelengths, the presence of any ad-

ditional absorber excepting HbO_2 and Hb can cause the underestimation or overestimation SaO_2 by reading SpO_2 . Influence degree depends on the absorption spectrum of the given absorber. If any pigmented component has a minimal extinction coefficient at 660nm as well as 940nm, then it has no effect on reliability of the spectrophotometric processing. Sometimes, the pathological concentrations of dyshemoglobins, such as methemoglobin MetHb and carboxyhemoglobin COHb, are present in arterial blood. For instance, COHb exists in blood because of carbon monoxide intoxication, or for heavy smokers. The pulse oximeter reading overestimates the true value of SaO_2 because COHb does not absorb at 940nm, however, its absorption is almost same to HbO_2 at 660nm.

3.3.2. Sensor design and application

1/ Action on object.

A risk of invasive influence is a very little. However, for an extended time of continuous monitoring, e.g. during a few hours or days, the used body site would be inspected. The sensors to be applied on neonates and small children require the special attention and control. This control would concern the surface of object near the emitting area of the photoemitter. The localized skin burn or injury could be observed as a consequence of the unsuitable application of the sensor or using of the unsuitable sensor to the given object.

2/ Shift in center wavelength of LEDs.

For the different intense and efficient LEDs of the same type, the variations in the center wavelength may be found to be up $\pm 15\text{nm}$ ⁷. In reality, the non-precise value of λ is of less importance at infrared region than that at red region because in the vicinity of 940nm the HbO_2 and Hb extinction curves are flatter. In red region, near 660nm, the HbO_2 curve is quite flat too, and the small shift in the center wavelength could be negligible. However, there is the steep shape of the Hb curve which can cause the worse accuracy of measurements at the low oxygen saturation. From the metrological point of view, it is advisable primarily to pair the proper specimens of R and IR LEDs in order to make conditions for photoemitter to operate effectively and reliably.

3/ Bad sensor set and sensor displacement.

The components of the optical part must be stable in their orientation with respect each other. Thus, the sensor design would be lightweight and comfortable, and useful to monitor the object at rest, e.g. unconscious patient, as well as in motion. Movements of whole sensor or displacement of its parts could cause a less effective transillumination up to an inability to the measurement realization.

Every sensor is made in purpose to apply on the specified body location and would be calibrated individually with the given pulse oximeter system.

3.3.3. Extraneous influences

Influence of the optical part environment mainly results from the sources of ambient optical radiation, such as sun, fluorescent and infrared lamps, and surgical xenon lamps. The photodetector receives any light reaching its photosensitive area. Thus, when the intensity of ambient light is very high, and this light propagates through object, or strikes directly the photodetector, then the utilized weak light coming from LEDs and transmitted by the object, can not be detected. The special technical procedures allow to compensate for these disturbances in the microprocessor part of measuring system. However, it is simple and effective to shield the sensor during monitoring in the rooms which are illuminated very intensely.

4. DISCUSSION AND CONCLUSIONS

Pulse oximetry corresponds to the current trends in medicine which demand to evolve the noninvasive and reliable diagnostic techniques. The oxygen saturation of arterial blood is defined in fact as the feature of the idealized absorbing medium different from the real object. Therefore, because the light processing in the optical part of the measuring system deviates the absorption laws, the obligatory formula of the resultant processing function would be established during calibration concerning the given device. In the paper some of problems dealing with reliability of processing to be realized in this part, have been described from the metrological point of view.

During empiric calibration the true values of $SaO_{2\%}$ are compared with the pulse oximeter readings $SpO_{2\%}$. This procedure requires drawing the samples of arterial blood and using of the standard invasive device, e.g. the multiwavelength co-oximeter. The standard data are obtained by inducing hypoxia in healthy volunteers breathing the various gas mixtures^{5,11}. It is difficult to obtain the reliable calibration data at saturation less than 60%-70%. Thus, the accuracy of the pulse oximeter readings tends to decrease during extreme hypoxia. For most of the produced now devices, messages concerning the $SpO_{2\%}$ reliability are given as follows :

Measurement range	: from 0 to 100%
Accuracy : $SaO_{2\%} \pm 1SD$	
Range from 100 to 50%	: $\pm 2\% + \pm 3\%$
Range from 50 to 0%	: unspecified
Resolution	: 1%

The lowest values of oxygen saturation can not be measured with known accuracy. Besides, all the presented disturbances especially affect the measurement procedure in this range. Fortunately, in the case of blood desaturation to know the precise value of measurement error is of less practical importance. Always, each of the readings which is equal to $SpO_{2\%} < 80\%$, is dangerous for patient and needs to undertake the intensive medical treatment. Therefore, it is helpful and advisable to measure not only the single values of $SpO_{2\%}$ but also to control its trend in order to detect when the desaturation impends over patient.

Authoress uses in her own studies, among the other things, the special design which may simulate and analyse the particular stages of processing occurring in the optical part of the pulse oximeter system^{13,15}. The constant and pulsatile components of the light signals transmitted by the object are converted to the measurable values of voltages. To creat the various specific measurement situations makes it possible to evaluate what factors and how much affect the processing reliability. If to observe the curve corresponding to the pulse waveform, then it becomes visible when the output signals from sensor are true and pure or rich in artifacts, or when these signals are only random. Further studies are in progress.

5. ACKNOWLEDGMENTS

I would like to thank Prof. J.W.Severinghaus from the Department of Anesthesia and the Cardiovascular Research Institute University of California in San Francisco for giving me his publications and many valuable informations which stimulated my interest in pulse oximetry.

Also, I wish to thank Prof. L.Wołowicka from the Department of Intensive Care Joint Hospital in Poznań, and Dr. A.Brzecka from the Antituberculitic and Lung Diseases Hospital in Wrocław for helpful discussions and enable me to do the clinical measurements.

6. REFERENCES

1. V.Twersky, Absorption and Multiple Scattering by Biological Suspensions", J.Opt.Soc.Am., vol.60, pp. 1084-1093, 1970.
2. D.O.Cooney, Biomedical Engineering Principles, vol.2, Marcel Dekker, Inc., New York, 1976.
3. M.J.Burke and M.V.Whelan,"Photoplethysmography: Selecting Optoelectronic Components", Med.Biol.Eng.Comp., vol.24, pp. 647-650, 1986.
4. R.N.Pittman, "In Vivo Photometric Analysis of Hemoglobin", Ann.Biom.Eng., vol.14, pp. 119-137, 1986.
5. J.W.Severinghaus and P.A.Astrup, History of Blood Gas Analysis, International Anesthesiology Clinics, Little,Brown and Co., Boston, 1987.
6. J.W.Severinghaus, "History, Status and Future of Pulse Oximetry", Adv.Exp.Med.Biol., vol.220, pp. 3-8, 1987.
7. J.A.Pologe, "Pulse Oximetry : Technical Aspects of Machine Design", Int.Anesthesiology Clin., vol.25, pp. 137-155, 1987.
8. M.J.C.van Gemert, S.L.Jacques, H.J.C.M.Sterenberg and W.M.Star, "Skin Optics", IEEE Trans.on Biom.Eng., vol.36, pp. 1146-1154, 1989.
9. K.K.Tremper and S.J.Barker, "Pulse Oximetry", Anesthesiology, vol.70, pp.98-108, 1989.
10. Y.Mendelson and J.C.Kent, "Variations in Optical Absorption Spectra of Adult and Fetal Hemoglobins and Its Effect on Pulse Oximetry", IEEE Trans.on Biom.Eng., vol.36,pp. 844-848, 1989.
11. J.W.Severinghaus, K.H.Naifeh and O.K.Shin, "Errors in 14 Pulse Oximeters During Profound Hypoxia", J.Clin.Monit., vol.5, pp. 72-81, 1989.
12. W.Cui, L.E.Ostrander and B.Y.Lee, "In Vivo Reflectance of Blood and Tissue as a Function of Light Wavelength", IEEE Trans.on Biom.Eng., vol.37, pp. 632-639, 1990.
13. A.Cysewska-Sobusiak, "Metrological Problems of Pulse Oximetric Measurements", Proceedings of 4th IMEKO TC-4 Int.Symposium on Intelligent Measurement of Electrical and Magnetic Quantities", pp. 104-109, Bulgarian Scientific and Technical Federation, Varna, 1990.
14. Y.Shimada, K.Nakashima, Y.Fujiwara, T.Komatsu, M.Kanishi, J.Takezawa and S.Takatani, "Evaluation of a New Reflectance Pulse Oximeter for Clinical Applications", Med.Biol.Eng.Comp., vol.29, pp. 557-561, 1991.
15. A.Cysewska-Sobusiak, "Model of Object to be Measured in Pulse Oximeter System" Proceedings of 5th IMEKO TC-4 Int.Symposium on Electrical Measuring Instruments for Low and Medium Frequencies", Vienna, 1992 (in press).

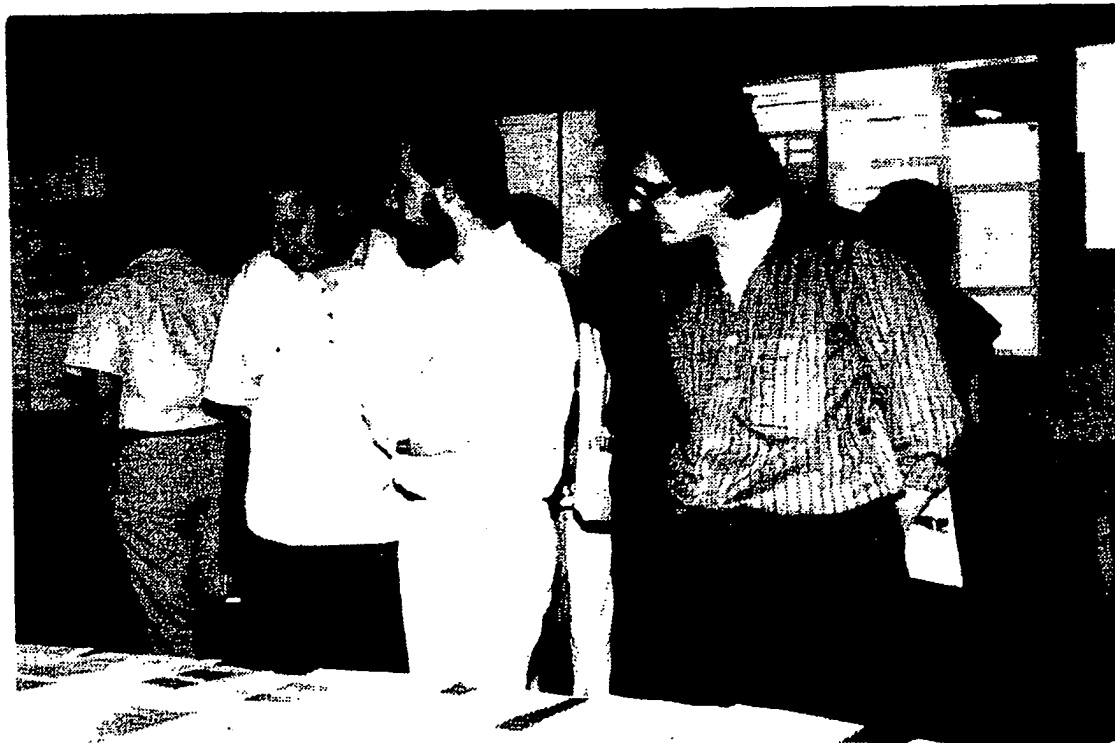
HIGH PERFORMANCE OPTICAL SPECTROMETRY

SPIE Volume 1711

SECTION 5

Varia

- TIR, nonlinear medium
- spectra of fractals



A group of conference participants at exhibiton of scientific books, journals and technical publications

HIGH PERFORMANCE OPTICAL SPECTROMETRY

SPIE Volume 1711



At the conference beginning Valentina Azarowa handed an original Russian mascot to the Conference Chairman with best wishes, which were then reinforced, in association with Igor V. Yevseyev (bottom left) and Kirill Prokhorov, at Get-Together Cocktail Party.

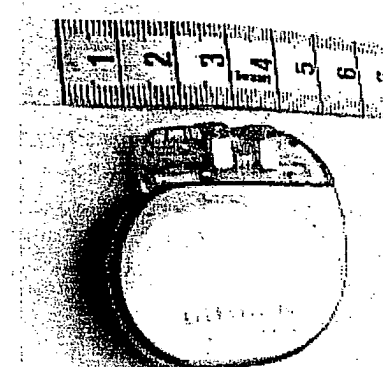


Artificial pacemaker

From Wikipedia, the free encyclopedia

This article is about a medical device which electrically stimulates the heart. For a similar device that stimulates the brain, see brain pacemaker.

A **pacemaker** (or "artificial pacemaker", so as not to be confused with the heart's natural pacemaker) is a medical device designed to regulate the beating of the heart. The purpose of an artificial pacemaker is to stimulate the heart when either the heart's native pacemaker is not fast enough or if there are blocks in the heart's electrical conduction system preventing the propagation of electrical impulses from the native pacemaker to the lower chambers of the heart, known as the ventricles.



A pacemaker

Contents

- 1 History of the implantable pacemaker
- 2 Applications
- 3 Methods of pacing
 - 3.1 External pacing
 - 3.2 Temporary internal pacing
 - 3.3 Permanent pacemaker placement
- 4 Basic pacemaker function
- 5 Bi-Ventricular Pacing (BVP)
- 6 Advancements in pacemaker function
- 7 Devices with pacemaker function
- 8 See also
- 9 References

History of the implantable pacemaker

The first external pacemaker was designed and built by the Canadian electrical engineer John Hopps in 1950. A substantial external device, it was somewhat crude and painful to the patient in use.

A number of inventors, including Paul Zoll, made smaller but still bulky external devices in the following years. The pacemakers built in the late 1950s were bulky, relied on external electrodes, and had to be plugged into a wall outlet. External electric shocks were frequently too traumatic for young heart block patients, and the AC-operated pacemaker could fail during a power blackout.

The first implantation into a human was made in 1958 by a Swedish team using a pacemaker designed by Rune Elmqvist and Åke Senning. The device failed after three hours. A second device was then implanted which lasted for two days. The world's first implantable pacemaker patient, Arne Larsson, survived the first tests and died in 2001 after having received 22 different pacemakers during his lifetime. In February 1960, an improved model relying on better materials was implanted in Montevideo, Uruguay. That device lasted until the patient died of other ailments, 9 months later. The early Swedish-designed devices used rechargeable batteries, which were charged by an induction coil from the outside.

Devices constructed by the American Wilson Greatbatch entered use in humans from April 1960 following extensive animal testing. The first patient lived for a further 18 months. The early devices suffered from battery

problems - every patient required an additional operation every 24 months to replace the batteries. Others who contributed significantly to the technological development of the pacemaker in the pioneering years were Bob Anderson of Medtronic Minneapolis, Geoffrey Davies of Devices Ltd in England, Barouh Berkovits and Sheldon Thaler of American Optical, Geoffrey Wickham of Telectronics Australia, Walter Keller of Cordis Corp. of Miami, Hans Thorander who joined previously mentioned Rune Elmquist of Elema-Schonander in Sweden, Janwillem van den Berg of Holland and Manuel A. Villafañá and Anthony Adducci of Cardiac Pacemakers Inc.

Applications

Artificial pacemakers can be used in order to help with and/or treat these conditions:

- Arrhythmias - an abnormal heartbeat including different types of heart block
- Sick sinus syndrome - when the sinoatrial node does not fire properly to contract the heart

Methods of pacing

External pacing

External pacemakers can be used for initial stabilization of a patient, but implantation of a permanent internal pacemaker is usually required for most conditions. External cardiac pacing is typically performed by placing two pacing pads on the chest wall. Usually one pad is placed on the upper portion of the sternum, while the other is placed along the left axilla, near the bottom of the rib cage. When an electrical impulse goes from one pad to the other, it will travel through the tissues between them and stimulate the muscles between them, including the cardiac muscle and the muscles of the chest wall. Electrically stimulating any muscle, including the heart muscle, will make it contract. The stimulation of the muscles of the chest wall will frequently make those muscles twitch at the same rate as the pacemaker is set. It was first invented by Canadian doctor John Hopps in 1950. He studied as an electrical engineer at the University of Manitoba.

Pacing the heart via external pacing pads should not be relied upon for an extended period of time. If the person is conscious, he or she may feel discomfort due to the frequent stimulation of the muscles of the chest wall. Also, stimulation of the chest wall muscles does not necessarily mean that the heart is being stimulated as well.

Temporary internal pacing

An alternative to external pacing is the temporary internal pacing wire. This is a wire that is placed under sterile conditions via a central venous catheter. The distal tip of the wire is placed into either the right atrium or right ventricle. The proximal tip of the wire is attached to the pacemaker generator, outside of the body. Temporary internal pacing is often used as a bridge to permanent pacemaker placement. Under certain conditions, a person may require temporary pacing but would not require permanent pacing. In this case, a temporary pacing wire may be the optimal treatment option.

Permanent pacemaker placement

Placement of a permanent pacemaker involves placement of one or more pacing wires within the chambers of the heart. One end of each wire is attached to the muscle of the heart. The other end is screwed into the pacemaker generator. The pacemaker generator is a hermetically sealed device containing a power source and the computer logic for the pacemaker.

Most commonly, the generator is placed below the subcutaneous fat of the chest wall, above the muscles and

bones of the chest. However, the placement may vary on a case by case basis.

The outer casing of pacemakers is so designed that it will rarely be rejected by the body's immune system. It is usually made of titanium, which is very inert in the body.

Basic pacemaker function

Modern pacemakers all have two functions. They listen to the heart's native electrical rhythm, and if the device doesn't sense any electrical activity within a certain time period, the device will stimulate the heart with a set amount of energy, measured in joules.

Bi-Ventricular Pacing (BVP)

A bi-ventricular pacemaker, also known as CRT (cardiac resynchronization therapy) is a type of pacemaker that can pace both ventricles (right and left) of the heart. By pacing both sides of the heart, the pacemaker can resynchronize a heart that does not beat in synchrony, which is common in heart failure patients. CRT devices have three leads, one in the Atrium, one in the right ventricle, and the last one is inserted through the coronary sinus to pace the left ventricle. CRT devices are shown to reduce mortality and improve quality of life in groups of heart failure patients.^{[1][2]}

Advancements in pacemaker function

When first invented, pacemakers controlled only the rate at which the heart's two largest chambers, the ventricles, beat.

Many advancements have been made to enhance the control of the pacemaker once implanted. Many of these enhancements have been made possible by the transition to microprocessor controlled pacemakers. Pacemakers that control not only the ventricles but the atria as well have become common. Pacemakers that control both the atria and ventricles are called dual-chamber pacemakers. Although these dual-chamber models are usually more expensive, timing the contractions of the atria to precede that of the ventricles improves the pumping efficiency of the heart and can be useful in congestive heart failure.

Rate responsive pacing allows the device to sense the physical activity of the patient and respond appropriately by increasing or decreasing the base pacing rate via rate response algorithms.

The DAVID trials^[3] have shown that unnecessary pacing of the right ventricle can lead to heart failure. New devices can keep the amount of right ventricle pacing to a minimum and thus prevent worsening of the heart disease.

Another advancement in pacemaker technology is left ventricular pacing. A pacemaker wire is placed on the outer surface of the left ventricle, with the goal of more physiological pacing than what is available in standard pacemakers. This extra wire is implanted to improve symptoms in patients with severe heart failure.

Devices with pacemaker function

Sometimes devices resembling pacemakers, called ICDs (implantable cardioverter-defibrillators) are implanted. These devices are often used in the treatment of patients at risk for sudden cardiac death. An ICD has the ability to treat many types of heart rhythm disturbances by means of pacing, cardioversion, or defibrillation.


[Home](#) • [Health Inform](#)
[Bradycardia](#)
[Diagnosis](#)
[Treatment](#)
[Management](#)

Treating Bradycardia

- [What is a Pacemaker?](#)
- [How a Pacing System Works](#)
- [Different Types of Pacing Systems](#)
 - > [Type: Single-chamber Pacing Systems](#)
 - > [Type: Dual-chamber Pacing Systems](#)
 - > [Type: Rate-responsive Pacing Systems](#)

[Medtronic's Pacing Systems](#)

[Surgery](#)

[Find a Physician/Specialist](#)

More Information about Bradycardia

- [Frequently Asked Questions](#)
- [Patient Stories](#)
- [Product Information](#)
- [Related Conditions](#)
 - > [Heart Block](#)
 - > [Sinus Node Dysfunction](#)
 - > [Tachyarrhythmia](#)
- [Information for Physicians](#)

Stages of Your Condition

- [Diagnosing Bradycardia](#)
- [Treating Bradycardia](#)
- [Managing Bradycardia](#)

[Important Safety Information](#)

[Email This Page to Friend or Family](#)

[Print This Page](#)

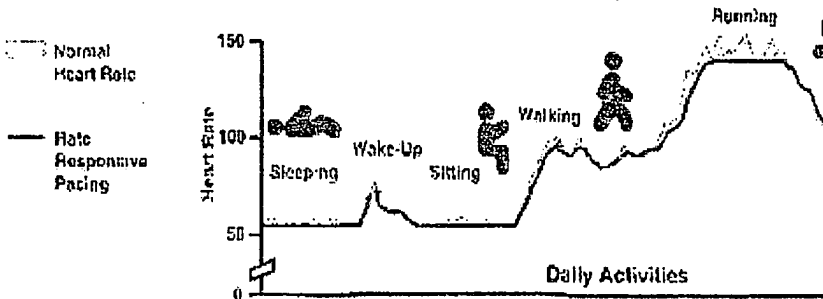
[Contact Medtronic](#)

Type: Rate-responsive Pacing Systems

A normal heart rhythm slows down or speeds up many times during the day. The heart beats slower while resting or sleeping. Exercise or excitement makes a heart beat faster because, in an excited state, the body requires greater amounts of oxygen. And, oxygen is brought to all parts of the body through the blood. When a heart is unable to adjust its pumping rate, a rate-responsive pacemaker is used.

A rate-responsive pacemaker mimics the heart's natural function of adjusting heart rate. A rate-responsive pacemaker uses one or more special sensors to recognize changes in how much blood and oxygen are needed by the body. Based on this information, the heart rate is adjusted to meet the body's changing needs for blood flow.

Adjusting Heart Rate to Activity



How Rate-responsive Pacemakers Function

A rate-responsive pacemaker uses one or more special sensors to detect changes in the body that indicate more oxygen is needed. Some sensors detect motion or how often you breathe. When a change is detected, the pacing rate is increased according to how the doctor programmed the pacemaker.

A pacemaker may have one or more sensors. The two most common are an activity sensor and a minute ventilation sensor.

Benefits of Rate-responsive Pacing

For people whose heart rate does not increase when needed, rate-responsive pacing:

The screenshot shows the main navigation bar and a central banner. The banner features the text "1948 - Present" above the "Energy Citations Database" logo. Below the banner are several links: Help, Full-Text Availability, Security/Disclaimers, Comments, DOE Information Bridge, EnergyFiles, OSTI Home, and energy.gov.

Availability information may be found in the Availability, Publisher, Research Organization, Resource Relation and/or Author (affiliation information) fields and/or via the "Full-text Availability" link. For a journal article, please see the Resource Relation field.

Title Effect of age and sex on bone density, bone mineral content and cortical index

Creator/Author Leichter, I. ; Weinreb, A. ; Hazan, G. ; Loewinger, E. ; Robin, G.C. ; Steinberg, R. ; Menczel, J. ; Makin, M.

Publication Date 1981 May 01

OSTI Identifier OSTI ID: 5431309

Other Number(s) CODEN: CORPA

Resource Type Journal Article

Resource Relation Clin. Orthop. ; Vol/Issue: 156

Subject 551000 -- Physiological Systems ;550800 -- Morphology; ;SKELETON-- DENSITY;SKELETON-- MORPHOLOGY; AGE DEPENDENCE;ANATOMY;BONE JOINTS;COMPARATIVE EVALUATIONS;FEMALES;MALES;MEASURING METHODS;MINERALS;PATHOLOGY;PHYSIOLOGY;QUANTITY RATIO;SEX DEPENDENCE

Related Subject BODY;ORGANS;PHYSICAL PROPERTIES;SKELETON

Description/ Abstract The density of cancellous bone in the nondominant radius of healthy subjects has been observed by the Compton scattering method as a function of age and sex.^The average density for males is higher than for females.^In males the density does not change up to the age of 80 years, while in females the density decreases beginning at age 50.^A significant decrease in the bone mineral content of the distal radius is observed at earlier ages as measured by the Cameron-Sorenson technique.^The average value of the cortical index of the third metacarpal shows some difference between the sexes over the age of 50, the index in males being higher than in the females.^Between 30 and 50 years the female cortical index is greater than in the males.^Little correlation was found among the three parameters studied, suggesting that they measure different phases of the pathophysiological processes involved in aging bone.

Country of Publication United States

Language English

Format Pages: 232-239

System Entry Date 2001 May 13



[About OSTI](#)

[Science.gov](#) • [First.gov](#) • [USAJOBS](#) • [Grants](#) • [Regulations.gov](#)



Last Updated: 12/12/2006

[ACP Medicine] [MedGer

[Latest](#) | [News](#) | [CME](#) | [Conferences](#) | [Resource Centers](#) | [Patient Ed.](#) | [Journals & Reference](#) | [Experts & V](#)[Search Medscape, MEDLINE and Drug Reference](#)[Search](#) | [Newsletters](#) | [Log Out](#)[Return to: Optimizing Treatment of Osteoporosis: Evolutions and Solutions](#)[CME Info](#) [Email this Article](#) [Print this Activity for Offline Reference](#)[Previous Page](#) | [Next Page](#)Target
LearninAu
DirAcc
StComm
Instr

Participa

Hardw
Rec

Pri

Con

CME i
indicat
educati
prof

Assessing Fracture Risk: Which Factors Are Clinically Most Important?

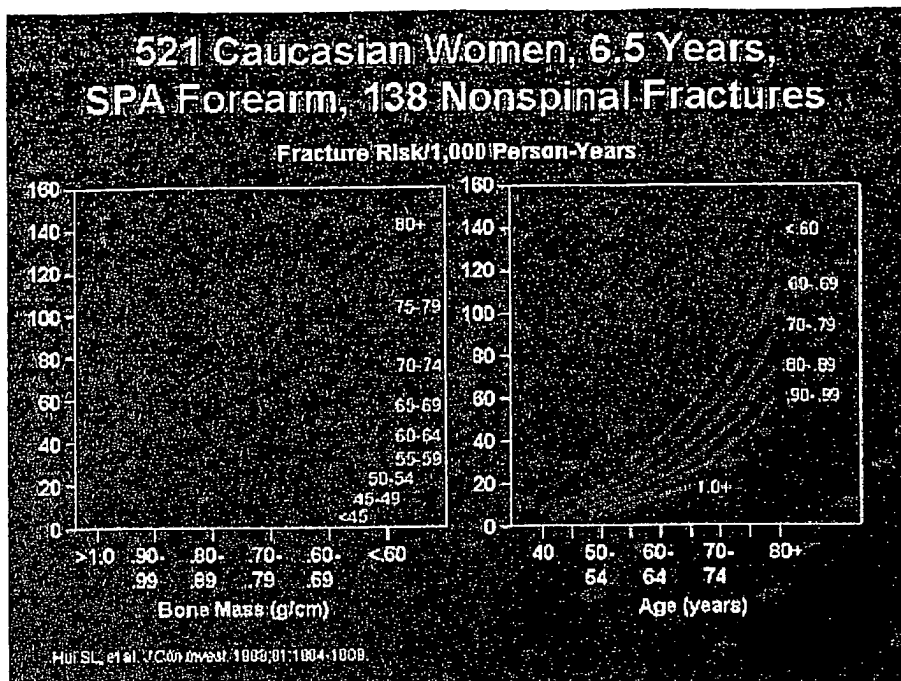
Paul D. Miller, MD

Increased Age Is a Risk Factor for Fracture



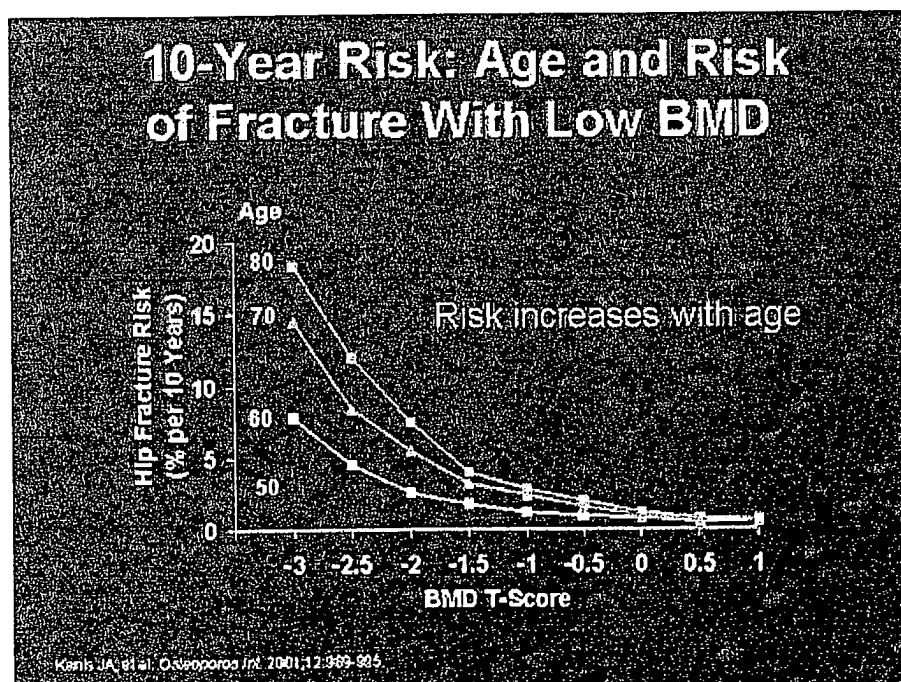
Slide 19. Increased Age Is a Risk Factor

One of the things that we need to put into this formula is age.



Slide 20. 521 Caucasian Women, 6.5 Years, SPA Forearm, 138 Nonspinal Fractures

This is the pivotal study. This was the landmark study published in 1988 in *Journal of Clinical Investigation* by Johnston's group, Dalsui and colleagues in Indianapolis at the University of Indiana. The slide shows forearm bone density and increased risk as a function of age. These are 138 nonspinal fractures over 6 and a half years. This was the first study to show that at the same level of BMD, let's take a number like 0.6 g/cm³; the risk from 50-59 is not very steep. I'll show you in NORA and I'll show you some other data, showing that fractures do occur in this. But the point is that even at the same level of bone density, the fracture risk is much greater as a function of age. Why is that? Part of it might be falling; older people fall more. But part of it is independent of falls. We can't quantitate that yet, but certainly there's something that happens to bone in terms of bone fragility, bone strength, that deteriorates in untreated people as they age. Some of those issues about bone quality are getting better defined by the basic science.



Slide 21. 10-Year Risk: Age and Risk of Fracture With Low BMD

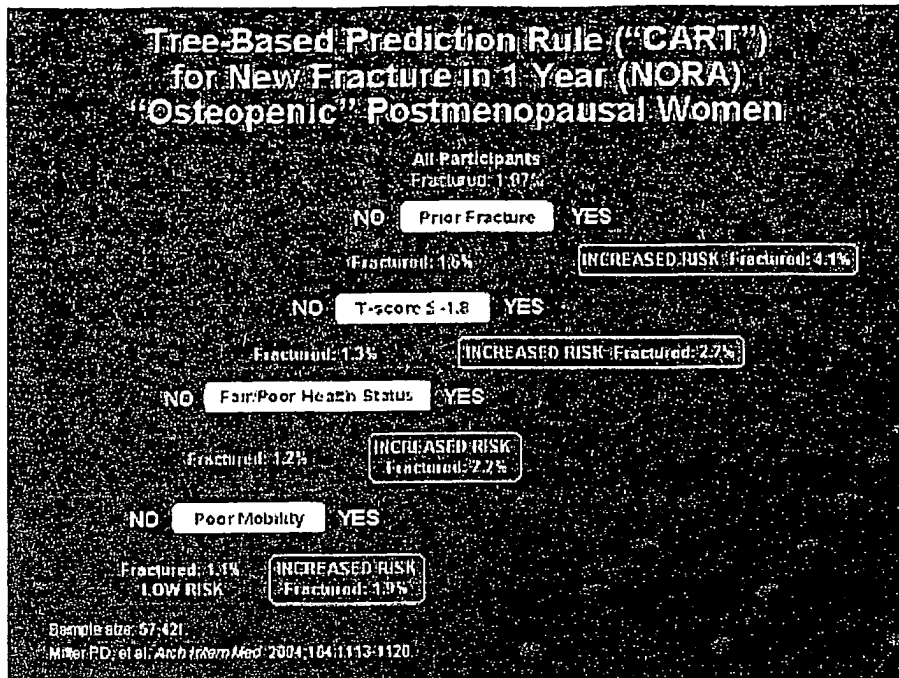
This is also the relationship between bone density and age for hip fractures over 10 years. Again, this is work from Professor Kanis. At age 80 we speak to patients differently about risk, but at age 50 we also speak about risk, even at the same level of BMD.

NORA: 1/3 of All Fractures and 1/5 of Hip Fractures Occurred in Women <65 Years Old*		
12-Month Follow-Up		
Age	50-64	65+
Osteoporotic Fractures		
# fractures	905	1,535
Fracture rate (95% CI)	8.4 (7.9, 9.0)	16.5 (15.6, 17.3)
% fractures	37%	63%
Hip Fractures		
# fractures	86	354
Fracture rate (95% CI)	0.8 (0.6, 1.0)	3.8 (3.4, 4.2)
% fractures	20%	80%

*Siris ES, et al. J Bone Miner Res. 2004;19:1215-1220.

Slide 22. NORA: One Third of All Fractures and One Fifth of Hip Fractures Occurred in Women < 65 Years Old

On the other hand, I want to point out a paper that was just published in the *Journal of Bone and Mineral Research*. Again, the lead author is Siris on the NORA data. They looked at the 12-month follow-up of fractures in NORA between the ages of 50-64 and 65 and older. You can see that the absolute risk of fractures in the younger age group is half the older age group. But it was still significant here – 37% of all the fractures that occurred in NORA occurred in 50- to 64-year-old people, and 86 of the 440 hip fractures occurred in this population. So even though the slope of the relationship between low bone density and age is shallower in 50- to 64-year-old people than the people above that age, these people still merit consideration because they have the risk for fracture.



Slide 23. Tree-Based Prediction Rule ("CART") for New Fracture in 1 Year (NORA) "Osteopenic" Postmenopausal Women

Until we can get the WHO-validated data completed, examined, and discussed, this is one of the attempts that we made to stratify the patients in the NORA data that were so-called osteopenic. The population in 1 year was 54,721. We published this in the *Archives of Internal Medicine*, and this is stratifying all of the risk factors by hierarchy, the highest risk to the lowest risk of the 32 risk factors that were captured in the NORA data set. By statistical analysis called classification and regression tree (CART), it ranks automatically from the highest to the lowest fracture risk. If you take a look at the top 4, any prior fracture in these populations after the age of 45 – it could be ankle fracture, pelvic fracture, forearm fracture, humeral fracture – was a predictor of risk; 4.1% of the population fractured again within 1 year, even those in the so-called osteopenic population. The T-score cut-off that predicted increased risk vs a risk in the overall population of about 1.2% was -1.8. That's not too far from the -2 in terms of treatment threshold recommended by the National Osteoporosis Foundation.

The next one validated by a number of other studies is a self-reported health status. If they reported that it was fair to poor there was an increased risk of poor mobility. If you combine a prior fracture after the age of 45 and low bone density, it captured 74% of the people that fractured in 1 year. This is an attempt to risk stratify, to be able to say we can't treat everybody at -1. We don't want to wait until everybody's -2.5. And maybe this is a way to look at this population in an intermediate level to predict risk.

Section 4 of 23

[Previous Page](#) [Next Page](#)

Search Medscape, MEDLINE and Drug Reference

[• About Medscape](#) [• Privacy & Ethics](#) [• Terms of Use](#) [• WebMD Health](#) [• WebMD Corp](#)

All material on this website is protected by copyright, Copyright © 1994-2006 by Medscape. This website also contains material copyrighted by Medscape requires Microsoft browsers in versions 6 or higher.

JOURNAL OF FORENSIC SCIENCES

Historical Backfile 1972-2005

Books & Journals/Journal of Forensic Sciences/Citation Page/

Volume 41, Issue 3 (May 1996)

ISSN: 0022-1198

[Click here to download this paper now for \\$25](#)

Published Online: 1 May 1996

Page Count: 9

[View License Agreement](#)

Attribution of Hand Bones to Sex and Population Groups

Smith, SL

Assistant Professor of Anthropology, Department of Sociology and Anthropology, University of Texas at Arlington, Arlington, TX.

Abstract

Forensic anthropologists assign sex and population group (race) to individuals on the basis of skeletal remains. While the most useful bones for these determinations are cranial and pelvic, these are not always available. The purpose of this paper is to provide models for classification using metacarpals and hand phalanges. Four samples of 40 individuals each (black and white males and females) form the dataset. Measurements include lengths and radioulnar and dorsopalmar widths of the 19 bones of each hand. The large number of total variables necessitated separate models for metacarpal and phalangeal categories; due to the considerable number of significant differences between corresponding right and left hand variables, separate models were created for right and left sides. A stepwise discriminant procedure was used to select variables, with some highly correlated ($r > 0.85$) variables subsequently removed. The model for left hand metacarpals has the greatest power of discrimination (89.4%); that for right hand middle phalanges, the least (71.7%). Metacarpals assign approximately 87–89%, proximal phalanges 76–79%, middle phalanges 72–79%, and distal phalanges 81–83% of individuals to their correct sex and population groups. Models exchanging variables selected from one side for corresponding variables on the other show discriminating power ranging from 72.3 to 85.6%. Thus roughly 70–90% of individuals are correctly classified by these models; more conservative “jackknife” estimates yield a success rate of approximately 67–82%. When these models are used for classification of sex alone, 89.9–94.4% (“jackknife” range, 88.7–94.4%) of cases are correctly classified; for race alone, 80.5–98.1% (“jackknife” range, 77.4–96.9%).

Keywords:

forensic anthropology, forensic science, historical skeletal remains, human identification, metacarpals, phalanges, physical anthropology